2.01 Uranium Oxide and MOX Production ☆

Masato Kato, Seiichiro Maeda, Tomoyuki Abe, and Koichi Asakura, Japan Atomic Energy Agency, Ibaraki, Japan

---

☆*Change History*: March 2016. Tomoyuki Abe and Koichi Asakura wrote original manuscript. March 2019. Masato Kato updated the basic properties for fuel pellet production and updated the reference list with some more up to date research. Seiichiro Maeda updated the outlook.
This is an update of Abe, T., Asakura, K., 2012. Chapter 2.15 – Uranium Oxide and MOX Production. In: Konings, R.J.M. (Ed.), Comprehensive Nuclear Materials, Elsevier, pp. 393–422.

Nomenclature

% TD   Theoretical density ratio
ABWR   Advanced boiling water reactor
ADU   Ammonium diuranate
AGR   Advanced gas cooled reactor
ATALANTE   Atelier Alpha et Laboratoires d'Analyses des Transuraniens et d'Etudes de retraitement, France
AUC   Ammonium uranyl carbonate
AUPuC   Ammonium uranyl plutonyl carbonate
BN   Belgonucléaire, Belgium
BNFL   British Nuclear Fuels plc, United Kingdom
BWR   Boiling water reactor
CANDU   CANadian Deuterium Uranium reactor
CFCa   Complexe de Fabrication de Cadarache, France
COCA   Cobroyage (co-milling) cadarache
COEX   CO-EXtraction
DNB   Departure from nucleate boiling
DOVITA   Dry reprocessing, oxide fuel, vibropac, integral, transmutation of actinides
FBR   Fast breeder reactor
FR   Fast reactor
HTR   High-temperature reactor
HWR   Heavy water reactor
IDR   Integrated dry route
ITU   Institute for Transuranium Elements, Germany
JAEA   Japan Atomic Energy Agency, Japan
LEFCA   Laboratoire d'Etudes et de Fabrications experimentales de Combustibles nucleaires Avancés, France

LWR   Light water reactor
MA   Minor actinide
MH method   Microwave heating denitration method
MH-MOX   Microwave heating denitrated MOX powder
MIMAS   Micronized master blend
MOX   Mixed oxide of uranium and plutonium
O/M ratio   Oxygen-to-metal ratio
OCOM   Optimized CO-milling
PCI   Pellet–cladding interaction
PCMI   Pellet–cladding mechanical interaction
PFFF   Plutonium Fuel Fabrication Facility, Japan
PFPF   Plutonium Fuel Production Facility, Japan
PVA   Polyethylene glycol or polyvinyl alcohol
PWR   Pressurized water reactor
R&D   Research and development
RIAR   Research Institute of Atomic Reactors, Russia
SBR   Short binderless route
SCK·CEN   Studiecentrum voor Kernenergie – Center d'Etude de l'énergie Nucléaire, Belgium
SEM   Scanning electron microscope
tHM   Tons of heavy metal
TIG   Tungsten inert gas
UKAEA   United Kingdom Atomic Energy Authority, United Kingdom
VHTR   Very high-temperature reactor
VVER   Vodo-Vodyanoi Energetichesky Reaktor (Russian type PWR)

Symbols

A Mass number
σ_a^{fast} Fast neutron absorption cross-section

$\sigma_a^{thermal}$ Thermal neutron absorption cross-section
σ_f^{fast} Fast neutron fission cross-section
$\sigma_f^{thermal}$ Thermal neutron fission cross-section

2.01.1   Introduction

Almost all the commercial nuclear power plants operating currently utilize uranium oxide fuel. These reactors, sometimes referred to as Generation II or Generation III reactors, produce 15% of the world's electricity supply. Production of the uranium oxide fuel required for these reactors is a mature industry and it annually requires more than 68,000 tU.[1] Fuel design differs according to the reactor types, which include the advanced gas cooled reactors (AGRs), pressurized water reactors (PWRs), boiling water reactors (BWRs), PWRs developed in the former Soviet Union (Vodo-Vodyanoi Energetichesky Reaktor, VVERs), and CANadian Deuterium Uranium (CANDU) reactors. There are some differences in the production processes to fit each fuel design. Plutonium utilization within the closed fuel cycle is essential to utilize natural uranium resources efficiently. Plutonium recycling demonstrations have been conducted in light water reactors (LWRs) and heavy water reactors (HWRs).[2] Industrial utilization of MOX in LWRs has commenced in some countries. The use of MOX in fast neutron reactors has many attractive features. Plutonium breeding in fast breeder reactors (FBRs) leads to drastically increased energy output from uranium

resources. Nuclide transmutation by fast neutrons to incinerate minor actinides (MAs) has the potential to reduce the long term radio-toxicity of spent nuclear fuel.

2.01.2　Basic Properties for Fuel Pellet Production

Oxide powders which are used as starting materials for oxide fuel production feed to a powder preparation process and then to a pelletizing process to get powder compacts, which are called green pellets. The green pellets undergo a dewaxing and sintering process to get sintered oxide pellets. Certain characteristics of the oxide powder and the sintered pellets are very important for fuel production. A brief summary of their important characteristics for pellet production is described in this section.

2.01.2.1　Phase Stability

Oxide nuclear fuels such as UO_2 and $(U,Pu)O_2$ have fluorite structure in which oxygen-to-metal (O/M) ratio equals 2.00. Plutonium and uranium atoms are both in metal sites forming a face centered cubic array. Oxygen atoms are placed at the center of the tetrahedral site of the metal atoms and form a simple cubic array. The actinide dioxides used as oxide nuclear fuels are oxygen nonstoichiometric compounds and stably exist in a large composition range. Uranium dioxide is stable in hyper-stoichiometric region and is used by adjusting O/M ratio to 2.00 in sintering process as fuels for LWR's. The $(U,Pu)O_2$ is stable in both regions of hyper and hypo-stoichiometric composition ranges. The O/M ratio in $(U,Pu)O_2$ which is used as an advanced nuclear fuel is adjusted to values lower than 2.00 in the sintering process to improve the compatibility between fuels and cladding materials.

In the UO_2-PuO_2 solid solution, phase transformation is not observed in temperature region up to melting temperature of about 3000K.[3] But phase separation to two fcc phases having different O/M ratios occurs in low temperature region of less than about 500K in hypo-stoichiometric MOX of more than 20% Pu content.[4,5] **Fig. 1** shows microstructure of $(U_{0.7}Pu_{0.3})O_{1.92}$ which have two fcc phases caused by phase separation. It is a concern that a phase separation might affect pellet production and irradiation behavior through micro crack generation in pellets. However, there are no observation of micro crack generation caused by such phase separation.

2.01.2.2　Theoretical Density

Fuel pellet density which relates to heat power of nuclear fuel pins is closely managed in fuel production process. The theoretical density which is the standard value to evaluate pellet density can be determined from lattice parameter, composition and isotopic composition. Lattice parameters can be described by Eq. (1),

$$a = 4/\sqrt{3} \cdot (r_c + r_a) \tag{1}$$

where a is the lattice parameter, r_c is the ionic radius of the cations and r_a is the ionic radius of the anions. Kato and Konashi[5,6] reported the equation to represent lattice parameter of hypo-stoichiometric MOX as a functions of O/M ratio, Pu content and minor actinide content. The theoretical density ρ_{th} of $(U,Pu)O_2$ varies as shown in **Fig. 2**. Theoretical density of $(U,Pu)O_2$ increases with increasing Pu content and decrease with decreasing O/M ratio.

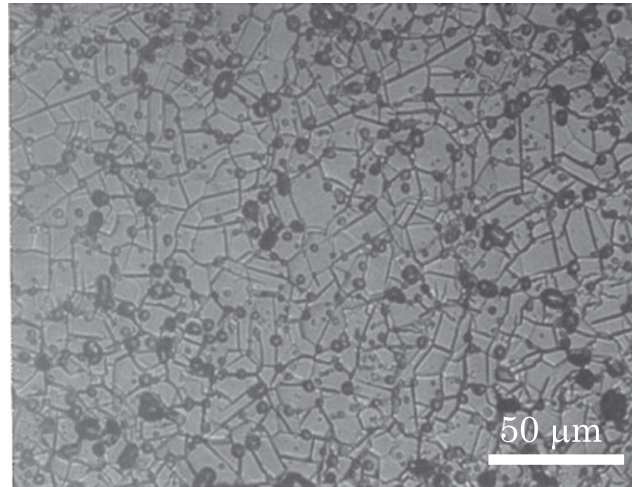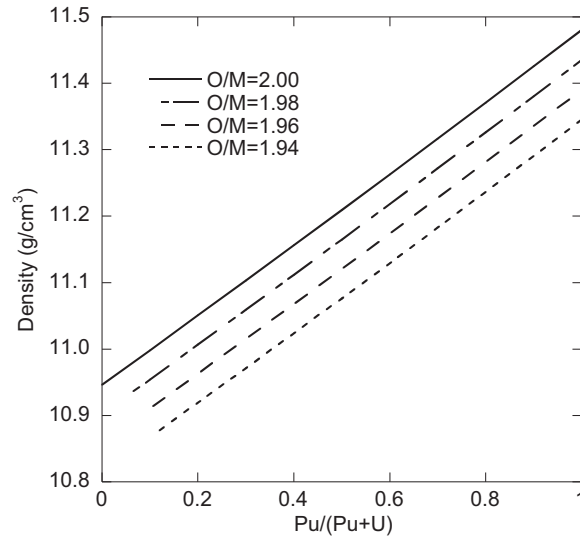**Fig. 1**　Microstructure of $(U_{0.7}Pu_{0.3})O_{1.92}$ having two fcc phases.

Fig. 2 Composition dependence of theoretical density of $(U,Pu)O_{2-x}$.

2.01.2.3 Effective Thermal Conductivity of MOX Powder

The temperature of MOX powder increases by self-heat generation by α-decay in storage and powdering steps in the fuel fabrication process. In MOX fuel fabrication process, the temperature increase in MOX powder should be prevented because the excessive temperature increase of MOX powder may possibly cause changes in powder characteristics (e.g., O/M ratio variation), degradation of additives (e.g., lubricant agents), and overheating of equipments in the fabrication process. An example of a preventive measure against the temperature increase of MOX powder is the use of a storage vessel that has radiator plates. The effective thermal conductivity of MOX powder is important for estimating its temperature distribution.

 The effective thermal conductivity of a powder can be defined as the combination of thermal conductivities of powder particles (with an effect of the O/M ratio on this conductivity), particle shapes, mean particle size, specific surface area and the atmospheric gas thermal conductivity, because the volume fraction of the atmosphere gas in the total volume is large.[7] **Fig. 3** shows the effective thermal conductivities of various MOX powders as functions of O/M ratio and bulk density.[7]

2.01.2.4 Flowability of Oxide Powder

In pellet fabrication, powder flowability is one of the most important characteristics to control the pellet density and determine the productivity of the fabrication process. It is well known that blended powders have very poor powder flowability, just after milling.[8] Therefore, the milled powder is granulated or mixed with a powder having good flowability to ensure uniform die filling and good compaction behavior.[8–10] Carr indices are a well-known method to evaluate powder flowability of dry solids.[11,12] The powder flowabilities of microwave heating denitrated MOX (MH-MOX) powder and ammonium diuranate (ADU) powder have been evaluated on the basis of Carr indices both before and after granulation.[13,14] The granulation increases flowability of the powder, improves the filling of the die and the pressing in the pellet production.

2.01.2.5 Sintering Behavior

Oxide fuel pellets are sintered in an atmosphere containing H_2 gas, and pellet density and O/M ratio are adjusted. Ratio of O/M is controlled by oxygen chemical potential $\Delta\overline{G}_{O2}$ which is calculated by,

$$\Delta\overline{G}_{O2} = RT \ln Po_2 \tag{2}$$

where R is the gas constant T is the temperature and P_{O_2} is the oxygen partial pressure in atmosphere. Considering the reaction of $H_2O = H_2 + 1/2O_2$, the equilibrium of the $H_2O–H_2$ system may be expressed by a formation free energy ΔG_f given by:

$$\Delta G_f = -RT \ln P_{H2O}/\left(P_{H2} \, P_{O2}^{1/2}\right) \tag{3}$$

 According to Eqs. (2) and (3), $\Delta\overline{G}_{O2}$ is determined by the ratio of P_{H2}/P_{H2O}, because ΔG_f is a fixed value known by previous experiments.[15] Relationship between $\Delta\overline{G}_{O2}$ and O/M ratio have been reported by many researchers.[15,16] Recently, Kato et al.[15] evaluated the latest experimental data set, and derived an equation to describe O/M ratio as a function of Pu content, P_{O2} and
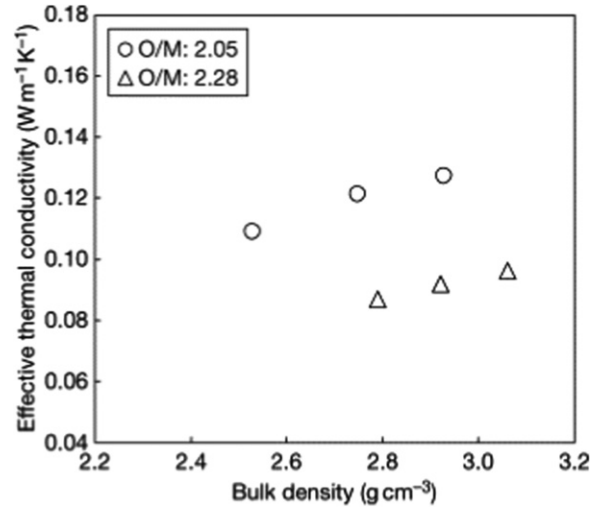
Fig. 3 Effective thermal conductivities of $(U_{0.5}Pu_{0.5})O_{2+x}$ powders. Reproduced from Takeuchi, K., Kato, M., Sunaoshi, T., Aono, S., Kashimura, M., 2009. J. Nucl. Mater. 385, 103–107.
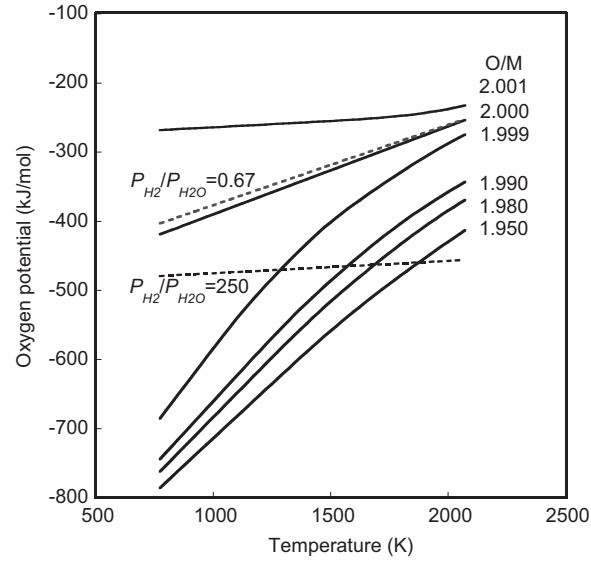
Fig. 4 Oxygen potential of $(U_{0.7}Pu_{0.3})O_{2\pm x}$ as functions of temperature and O/M ratio.

temperature as follows,

$$O/M = 2 - \left\{ \left(\exp\left(\frac{44.0 + 55.8 \cdot C_{Pu}}{R}\right) \cdot \exp\left(-\frac{376,000}{RT}\right) \cdot P_{O_2}^{-1/2} \right)^{-5} \right.$$
$$+ \left(\left(\exp\left(\frac{68.8 + 1313.3 \cdot C_{Pu}}{R}\right) \cdot \exp\left(\frac{515,000}{RT}\right) \right)^{1/2} \cdot P_{O_2}^{-1/4} \right)^{-5}$$
$$+ \left(\left(2 \cdot \exp\left(\frac{153.5 - 96.5 \cdot C_{Pu} + 331.0 \cdot C_{Pu}^2}{R}\right) \cdot \exp\left(-\frac{891,000}{RT}\right) \right)^{1/3} P_{O_2}^{-1/3} \right)^{-5}$$
$$\left. + \left(\frac{1}{2} C_{Pu}\right)^{-5} \right\}^{-1/5} + \left\{ \exp\left(\frac{-22.8 - 84.5 \cdot C_{Pu}}{R}\right) \cdot \exp\left(\frac{105,000}{RT}\right) \cdot P_{O_2}^{1/2} \right\}, \tag{4}$$

where C_{Pu} is the Pu content, R is the gas constant and T is the temperature. **Fig. 4** shows oxygen potential of $(U_{0.7}Pu_{0.3})O_{2\pm x}$ for x between -0.05 and $+0.001$, and oxygen potential changes of $P_{H2}/P_{H2O} = 0.67$ and 250 are shown with broken lines. For

Fig. 5   Change of O/M ratio during sintering in an atmosphere with $P_{H2}/P_{H2O} = 250$.

Fig. 6   Densification of $(U_{0.7}Pu_{0.3})O_{2.00}$ and $(U_{0.7}Pu_{0.3})O_{1.99}$.

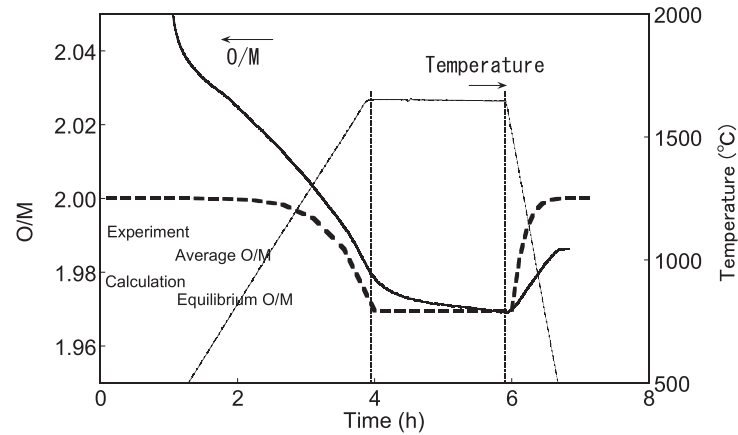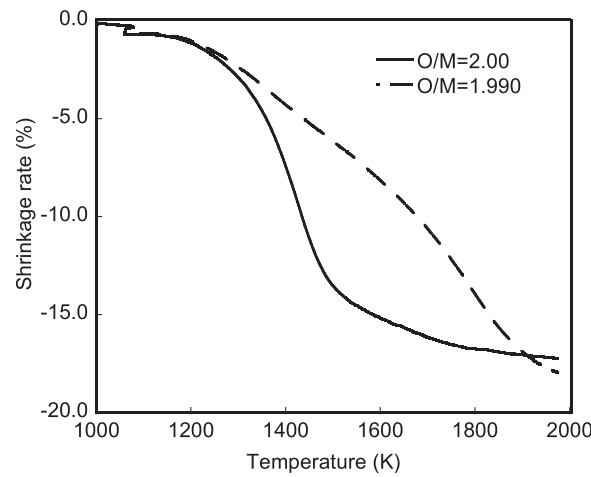$P_{H2}/P_{H2O} = 0.67$, O/M ratio equals 2.00 in a wide temperature range. In an atmosphere with $P_{H2}/P_{H2O} = 250$, MOX reduction increases with increasing temperatures. The change of O/M ratio measured during sintering in an atmosphere with $P_{H2}/P_{H2O} = 250$ is shown in **Fig. 5**. Equilibrium O/M ratio is shown with broken line. A pressed pellet prepared from powder of O/M = 2.10 was used in these measurements. It can be seen that the O/M ratio of the sample approaches the equilibrium O/M ratio.

Shrinkage behavior has been investigated by many researchers, and it was shown that shrinkage rate significantly change depending on the sintering atmosphere gas. **Fig. 6** shows shrinkage rate of $(U_{0.7}Pu_{0.3})O_{2.00}$ and $(U_{0.7}Pu_{0.3})O_{1.99}$ when sintered in P_{O2}-controlled atmosphere. Shrinkage rate of $(U_{0.7}Pu_{0.3})O_{2.00}$ is higher than that of $(U_{0.7}Pu_{0.3})O_{1.99}$. The typical sintering process of MOX pellets is carried out at around 1973K in a reduced atmosphere. Tekeuchi *et al.* investigated by dilatometry the sintering behavior of $(U_{0.8}Pu_{0.2})O_{2\pm x}$ pellets as a function of P_{H2}/P_{H2O} ratio in the furnace atmosphere.[17] They found out that diffusion process was dominant in the sintering of MOX with O/M = 2.00, and that the sintering was observed in the lower temperature region of 1200–1600K lower than with low O/M MOX pellets. Thus, sintering behavior of MOX pellets is significantly affected by O/M ratio.

2.01.2.6   Oxidation of Low O/M Pellet

It was reported that the oxidation rate of low O/M pellets in air is very fast even around room temperatures.[18,19] Suzuki *et al.*[19] investigated the oxidation rate of low O/M pellets. They analyzed the oxidation by diffusion-controlled process and estimated the activation energy of the chemical diffusion to be 73.4 kJ/mol. **Fig. 7** shows experimental results of oxidation rate measurements at 333 and 358K. If $(U_{0.7}Pu_{0.3})O_{2-x}$ pellets are kept at 313K for 100 days, their O/M values will increase by 0.015 and may attain O/M = 2.00.

Generally, the MOX pellets are kept in a glove box for a few months until the pellets are fabricated into fuel pins. Therefore, a cooling system to keep temperatures lower than 300 K is needed to maintain the low O/M values of the stored pellets, particularly
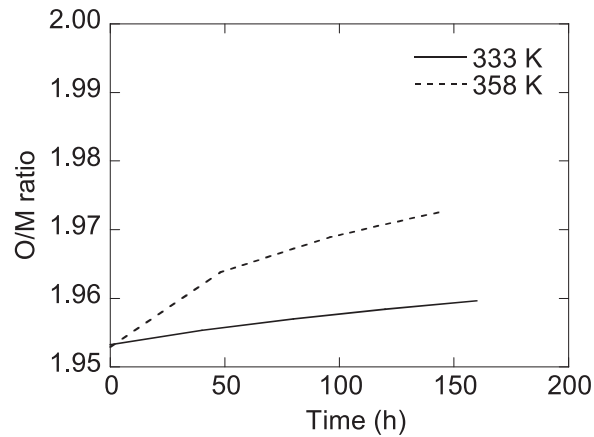
Fig. 7 Oxidation rate of low O/M MOX pellet at 333 and 358K.
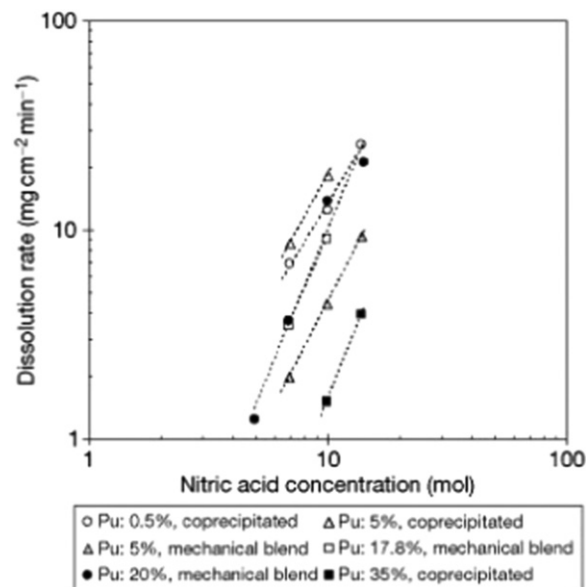
Fig. 8 Dissolution rate of mixed oxide of uranium and plutonium with various Pu contents as a function of the nitric acid concentration. Reproduced from Oak Ridge National Laboratory, 1965. Dissolution of High-Density UO_2, PuO_2, and UO_2–PuO_2 Pellets in Inorganic Acids. ORNL-3695. Oak Ridge, TN: Oak Ridge National Laboratory.

for fast reactor stainless steel pins in which initial hypo stoichiometry is needed to reduce or avoid internal corrosion of the cladding (see article on fast reactor fuel behavior – M. Pelletier in this second edition).

2.01.2.7 Solubility in Nitric Acid Solution

When the nuclear fuel cycle is considered, the dissolution of oxide fuel is the essential first step in aqueous reprocessing. The solubility and dissolution rate of oxide fuel in nitric acid solution are important parameters related to the capabilities of the reprocessing process. Generally, it has been supposed that the dissolution of MOX fuel decreases with an increase in the plutonium content. The maximum plutonium content of MOX driver fuel for fast reactors has been limited to about 30%, from the viewpoint of solubility in nitric acid solution.

There have been many studies on the solubility of oxide fuel in nitric acid solution.[20–23] From the results of these studies, it has been supposed that the factors affecting the dissolution rate of MOX are the fuel fabrication conditions (homogeneity of the admixture of UO_2 and PuO_2, sintering conditions and plutonium content, etc.) and the fuel dissolution conditions (nitric acid concentration, solution temperature, dissolution time, etc.) (see **Fig. 8**).

Table 1   Half lives and typical reaction cross sections of isotopes in MOX fuel

Nuclide	Half life (year)	Cross-section (barn, 10^{-28} m^2)				Specific power from decay (W kg^{-1})
		$\sigma_a^{thermal}$	$\sigma_f^{thermal}$	σ_a^{fast}	σ_a^{fast}	
^{235}U	7.04E + 08	684	585	2.49	1.95	8.7E − 05
^{238}U	4.47E + 09	2.7	1.20E − 05			1.2E − 05
^{238}Pu	87.74	558	17.9			820
^{239}Pu	2.41E + 04	1018	747	2.3	1.83	2.8
^{240}Pu	6564	289	5.90E − 02			10.2
^{241}Pu	14.35	1374	1012	2.86	2.45	12.4

Source: Shibata, K., *et al.*, 2002. J. Nucl. Sci. Technol. 39, 1125–1136. Hori, M., 1993. Kiso Kousokuro Kougaku (Basic Fast Reactor Engineering). Tokyo: The Nikkan Kogyo Shimbun (in Japanese).

2.01.2.8   Nuclear Characteristics of Uranium and Plutonium Isotopes

Plutonium is an isotopically composition-variable material and the variation is attributable to its generation reaction in LWR fuel, the initial uranium enrichment and burn-up of the LWR fuel, and so forth. It needs various methodologies and much prudence in its handling because its nuclear properties differ noticeably from one isotope (nuclide) to another. **Table 1**[24,25] summarizes the principal nuclear properties of typical nuclides in MOX fuel, including uranium isotopes. A material with a high content of ^{238}Pu is more calorific owing to its decay mode (α) and short life. Therefore, the content in ^{238}Pu is a limiting factor for handling large batch sizes in a fabrication process. ^{241}Pu, which also has a short life, causes alteration in the isotopic composition even during a relatively short period, for example, during storage after fuel fabrication but before loading into a reactor. Besides the above, neutron reaction cross-sections are completely different in isotopes and reactor types. In the MOX fuel fabrication, the Pu content must be adapted, to secure sufficient in-core reactivity, taking such variations in the cross-sections into consideration.[26]

The nuclear characteristics of uranium and plutonium are needed for the evaluation of radiation exposure during the fuel fabrication process. In particular, the short life of a nuclide merits attention with regard to exposure to radiation. All isotopes listed in **Table 1** are α-emitters, especially ^{238}Pu, which has highly significant α-radioactivity. ^{241}Am, which is adjunct to ^{241}Pu, is also a strong α-emitter. These two nuclides also give off strong γ-ray emissions following their α-decay. The major sources of neutrons are the even-A (mass number) plutonium isotopes such as ^{238}Pu, ^{240}Pu, and ^{242}Pu because of their high probability for spontaneous fission. In addition, especially in oxide fuels such as MOX fuel, α-particle bombardment of oxygen isotopes is an important factor that determines neutron emission. ^{238}Pu and ^{241}Am have a higher specific (per unit mass) influence on this reaction than other nuclides because of their large α-ray emission rates, as mentioned above. In addition, these two nuclides have a somewhat higher Q-value (α-ray energy) for decay and this increasingly affects the neutron production rate.

Turning to the topic of safeguards, the large neutron yield by spontaneous fission from the MOX fuel is utilized for a neutron coincidence counting method for inventory verification. This method uses the fact that neutrons from spontaneous fission or induced fission are essentially emitted simultaneously. This measurement can be made in the presence of neutrons from room background or (α, n) reactions because these neutrons are noncoincident, or random, in their arrival times. The detection signals of these neutrons are analyzed to determine each plutonium isotope quantity.

Burnable poison suppresses initial fuel reactivity during fuel life and compensates fuel reactivity with the gradual reduction in burnable poison with burn-up. Consequently, the fuel burn-up reactivity is lowered and this lowered reactivity leads to an extended operation cycle period. Burnable poison is often mixed into oxide fuel. Gadolinium is a typical one; it has a variety of stable and substable isotopes and some of them ($^{155,157}Gd$) have large thermal capture cross-sections. They are used in the form of a solid solution $(U,Gd)O_2$ during sintering.

2.01.3   Fuel Design[2,27–29]

2.01.3.1   Fuel Rod Design

2.01.3.1.1   Basic structural design

In LWRs and FBRs, a number of fuel rods are formed into a fuel assembly. The fuel rod is a barrier (containment) for fission products; it has a circular cross-section that is suited for withstanding the primary pressure stress due to the external pressure of the coolant and the increase in internal pressure by fission gas release. An axial stack of cylindrical fuel pellets is encased in a cladding tube, both ends of which are welded shut with plugs. A gas plenum is located at the top part of the rod, in most cases, to form a free space volume that can accommodate internal gas. Helium gas fills the free space at atmospheric pressure or at a given pressure. The choice of this inert gas was made due to its high thermal conductivity compared to the other inert gases. A hold-down spring, located in the gas plenum, maintains the fuel stack in place during shipment and handling. UO_2 insulator pellets are inserted at both ends of the fuel stack, in some fuel designs, to thermally isolate metallic parts such as the end plug and the hold-down spring.

Table 2   Summary of fuel rod design specifications for LWRs and CANDU reactors

Reactor type	PWR	BWR	VVER	CANDU
Fuel assembly type	Mitsubishi 17 × 17	GNF 9 × 9A	TVS-2M	AECL 28-element
No. of fuel rod per assembly	264	66 + (8)[a]	312	28
Rod length (mm)	3856	4090 (2600)[a]	3988	493
Rod diameter (mm)	9.5	11.2	9.1	15
Pellet material	UO_2	UO_2	UO_2	UO_2
Pellet diameter (mm)	8.19/0	9.6/0	7.6/1.2	14/0
Pellet density (g cm^{-3})	97% TD	97% TD	10.4–10.7	10.6
Clad material	MDA[b]/Zirlo	Zry-2 (Zr-liner)	Zr–1% Nb	Zry-4
Clad thickness (mm)	0.57	0.71	0.63	0.4
Average discharge burn-up (MWd kg HM^{-1})	55	45	60	8

[a]Partial length rod.
[b]Mitsubishi developed alloy.
Source: Tarlton, S., 2008. Nucl. Eng. Int. 53, 26–36.

2.01.3.1.2   Fuel rods for LWRs

Table 2 summarizes LWR fuel rod design specifications.[30] LWR UO_2 fuel rods contain dense low-enrichment UO_2 pellets in a zirconium alloy cladding; they are operated at a low linear heat rate with centerline temperatures normally below 1400°C. The fuel pellets of the VVER have a small central hole (1.2–1.4 mm in diameter).

Fission gas release is low under these conditions and no large gas plenum is needed. Burnable absorber fuel rods containing $(U,Gd)O_2$ pellets are located in some part of the fuel assemblies of LWRs to flatten reactivity change throughout the reactor operation cycle.

Great efforts have been made in LWR fuel rod design in order to achieve the following good performance features: high burn-up, long operation cycle, good economy, and high reliability. Toward achieving these ends, many modifications have been made, such as the development of high-density UO_2 pellets, axial blankets for reducing neutron leakage, ZrB_2 integral burnable absorber, high Gd content UO_2–Gd_2O_3 pellets, corrosion-resistant cladding materials, and optimization of helium pressure and plenum length in the rod designs.

LWR MOX fuel rods contain MOX pellets that have a low plutonium content. As the plutonium concentration is low, their irradiation behavior is similar to that of LWR UO_2 fuel rods. No additional problems are apparent, with the possible exception of higher gas release and therefore an increase in rod internal pressure at high burn-up. Power decrease with burn-up is lower in the MOX fuel than in UO_2 fuel because of the neutronic properties of the plutonium isotopes and thus MOX fuel is irradiated at higher power later in its life, releasing more fission gases. In addition, the slightly lower thermal conductivity of MOX may give rise to higher fuel temperatures, resulting in higher fission gas release. Design changes, such as lowering the helium filling pressure, increasing the plenum volume, and/or decreasing the fuel stack length in the rod, are applied to accommodate higher gas release in MOX fuel rods.

2.01.3.1.3   Fuel rods for CANDU reactors and AGRs

CANDU reactors and AGRs generally have fuel rod design specifications similar to those of LWRs. The CANDU reactors use natural uranium oxide or slightly enriched uranium oxide contained within a thin Zircaloy clad, and design burn-up is lower than that of LWRs. In AGR fuel rods, uranium dioxide pellets, enriched to about 3%, are encased in a stainless steel clad. Fuel bundles of both reactors have circular, cylindrical shapes to fit in the pressure tube of CANDU reactors or in the graphite sleeve of AGRs. The fuel rod diameter differs according to the number of fuel rods per bundle. Typical CANDU fuel rod design specifications for a 28-rod bundle are presented in **Table 2**.[30] The overall fuel rod lengths of both reactor types are much shorter than those of LWRs in order to fit their fuel assembly design which enables on-load refueling.

2.01.3.1.4   Fuel rods for FBRs

FBR fuel rods contain MOX pellets having high plutonium content, with the exception of Russian FBRs, BN-350, and BN-600 in which high enrichment UO_2 fuel pellets have been mostly used. Fuel pellets of less than 8 mm diameter are encased in a stainless steel cladding; they operate at a high linear heat rate with centerline temperatures of around 2000°C or higher. Under these conditions, fission gas release is typically high ($> 80\%$) and a very large plenum is included to limit gas pressure. The gas plenum is located at the bottom of the rod in some fuel designs, aimed at minimizing plenum length, thanks to the lower gas temperature at the bottom of the rod. Upper and lower sections of depleted UO_2 pellets are included for breeding. Pellet-smeared density is set not to exceed a criterion that is formulated as a function of burn-up to avoid fuel–cladding mechanical interaction at high burn-up; high-density annular pellets or low-density solid pellets are used; the former lower the fuel centerline temperature allowing a higher linear heat rate preserving the necessary margin to fuel fusion.[31]

2.01.3.1.5   *Fissile content of oxide pellets*

The same U enrichment is used throughout a given PWR fuel assembly, but the core usually contains several levels of enrichment arranged to give uniform power distribution. In contrast, BWR fuel rods have several axial segments with different enrichments and a BWR fuel assembly has several different rods with different enrichments. Thus, there are a variety of UO_2 pellets with different U enrichments depending on reactor design; the enrichments are within 5% which is due to the limits of fuel fabrication facilities and fuel shipments.

For current LWR MOX fuels, depleted uranium (0.2%–0.3% ^{235}U), which is obtained in the form of tails from the enrichment process, is coupled with plutonium because there are economic incentives to concentrate as much plutonium in as few fuel assemblies as possible as it conserves the expensive fabrication cost of MOX fuel. As the quality of plutonium, from a neutronic aspect, varies with the isotope composition of plutonium, the specification of the plutonium content of LWR MOX fuel is affected by the quality of plutonium.

To determine plutonium content of FBR MOX fuel, equivalent ^{239}Pu ($^{239}Pu/(U + Pu)$) is used. The actual plutonium content for a given batch is obtained by a calculation that uses the neutronic equivalent coefficient of each isotope and the isotope composition of plutonium to be used for the batch. ^{241}Am, a daughter product of ^{241}Pu, is considered in the calculation as well. The specification for equivalent ^{239}Pu ($^{239}Pu/(U + Pu)$) is relatively low for a large size core; equivalent ^{239}Pu is 12%–15% for the SUPERPHENIX (1200 GWe),[28] 14%–22% for MONJU (280 GWe).

2.01.3.2   Fuel Assembly Design

2.01.3.2.1   *PWR UO_2 fuel assembly*

Fig. 9 (see "Relevant Website") shows an example of a PWR fuel assembly. PWRs have 197–230 mm square, ductless assemblies that traverse the full 2635–4550 mm height of the core. They comprise a basic support structure of unfueled zirconium alloy guide tubes attached to the top- and bottom-end fittings, an array of 14×14–18×18 fuel elements (minus the number of guide tubes), and several axially spaced grids that hold the array together. About half of the assemblies have rod control clusters attached at their upper end; these consist of 18–24 slender stainless-steel-clad absorber rods of AgInCd alloy or B_4C, individually located in the guide tubes. The absorber rods are withdrawn for startup and are repositioned after refueling; the reactor is controlled at power by altering the concentration of an absorber (boric acid) in the coolant. The bottom-end fitting is located on the core grid plate and the assembly is spring loaded against a hold-down system to compensate for differential expansion or growth during irradiation.

Fine control is obtained by incorporating a burnable poison like gadolinium in some of the fuel pins, in which it is admixed with UO_2 in the core region, and with the upper and lower sections of natural UO_2. By minimizing power changes in this manner, the
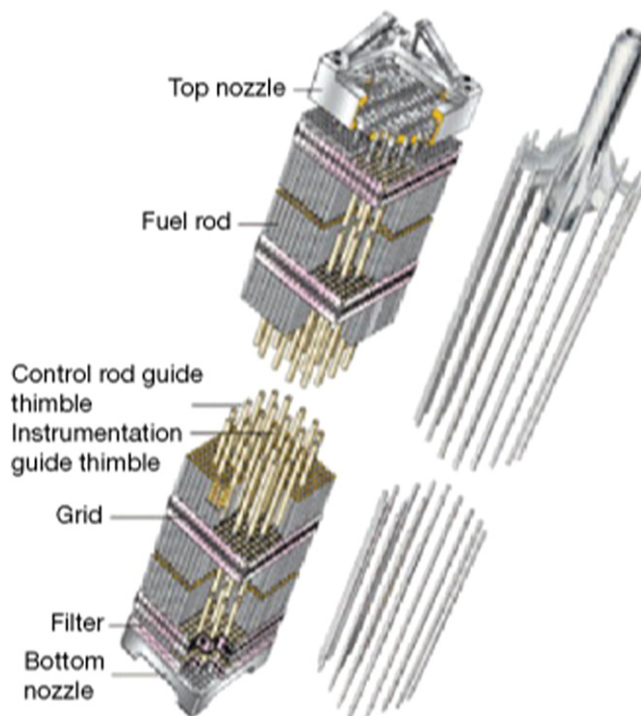

Fig. 9   Example pressurized water reactor fuel assembly design of the $17 \times 17 - 24$ type with a fuel assembly averaged U enrichment of 3.9%. Reproduced from available at: http://www.mhi.co.jp/en/index.html.
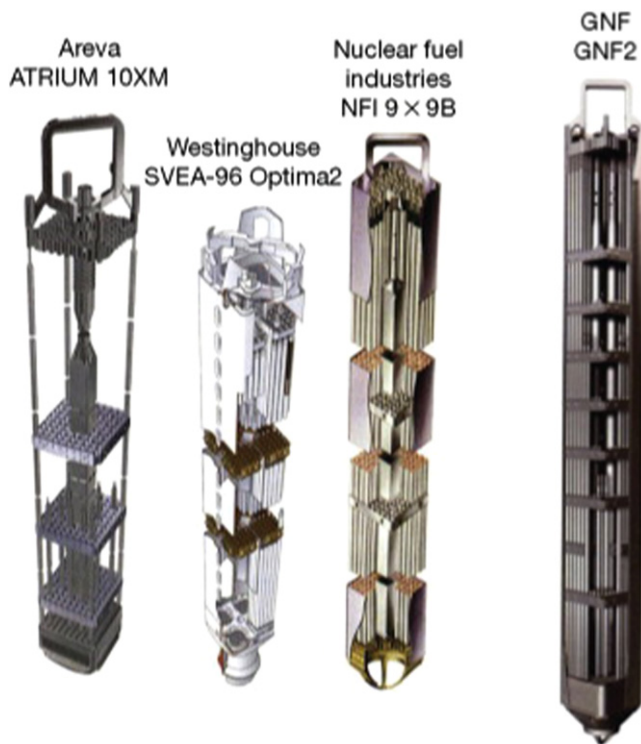
Fig. 10 Example boiling water reactor fuel assemblies. Reproduced from Tarlton, S., 2008. Nucl. Eng. Int. 53, 26–36.

incidence of pellet–clad interaction (PCI) failures can be kept to very low, acceptable values. Various improvements in fuel assembly design have been adopted. To improve reliability, for instance, debris filtering was adopted in the structural design of the bottom part of the fuel assembly, the grid structure design was modified against fretting corrosion, and an intermediate flow mixer grid was added to enhance the margin to depart from nucleate boiling (DNB). Zirconium alloy grids for better neutronics, optimized distribution of fissile and fertile materials, and a burnable poison to improve fuel cycle economy and to extend reactor cycle length were all introduced for economy in the current assembly designs, as also the removable top nozzle to reduce operation and maintenance costs.

2.01.3.2.2   BWR UO_2 fuel assembly

Fig. 10[30] shows some examples of BWR fuel assemblies. BWRs have 110–140 mm square full-core height assemblies which, unlike their PWR counterparts, are contained within thick-walled channel boxes of zirconium alloy. They contain arrays of 6 × 6–10 × 10 fuel elements, usually with eight elements acting as tie rods that screw into upper and lower tie plates. Some of the element positions are occupied by unfueled water-filled tubes (called water rods) or water channels and are used to control local flux peaking. Element separation is maintained by grid spacers that are attached to the water rods and evenly distributed along the entire length. The square duct is attached to a top-end fixture, relative to which the remainder of the subassembly may slide. The bottom-end fitting has a mechanized orifice to control flow in the subassembly and this is located in the core grid plate. The upper end fixture has a handle for loading and unloading against which the hold-down bars rest to prevent levitation.

There are no absorber elements in BWR assemblies and reactor control is achieved by having cruciform-shaped absorber blades throughout the core which move vertically in the clearance between sets of four subassemblies. Power peaking is minimized on the local scale by having fuel elements with different enrichments and burnable poisons (generally Gd) dispersed within each assembly. Various fuel design improvements have been adopted, such as a debris-filtering structure for better reliability, optimized distribution of water channels, fissile material with partial length fuel rods and burnable poison use to improve fuel cycle economy and to extend reactor cycle length.

2.01.3.2.3   VVER fuel assembly

Fig. 11[30] shows an example of a VVER fuel assembly. The VVER uses hexagonal fuel assemblies of 3200–4690 mm length and 145–235 mm width. The assembly is used such that it is contained in a hexagonal shroud, but shroudless assemblies are available for the VVER-1000.[30]

2.01.3.2.4   CANDU reactor fuel

Fig. 12[30] shows an example of a CANDU fuel bundle. Twelve fuel bundles fit within each fuel channel that is horizontally aligned in the reactor core.
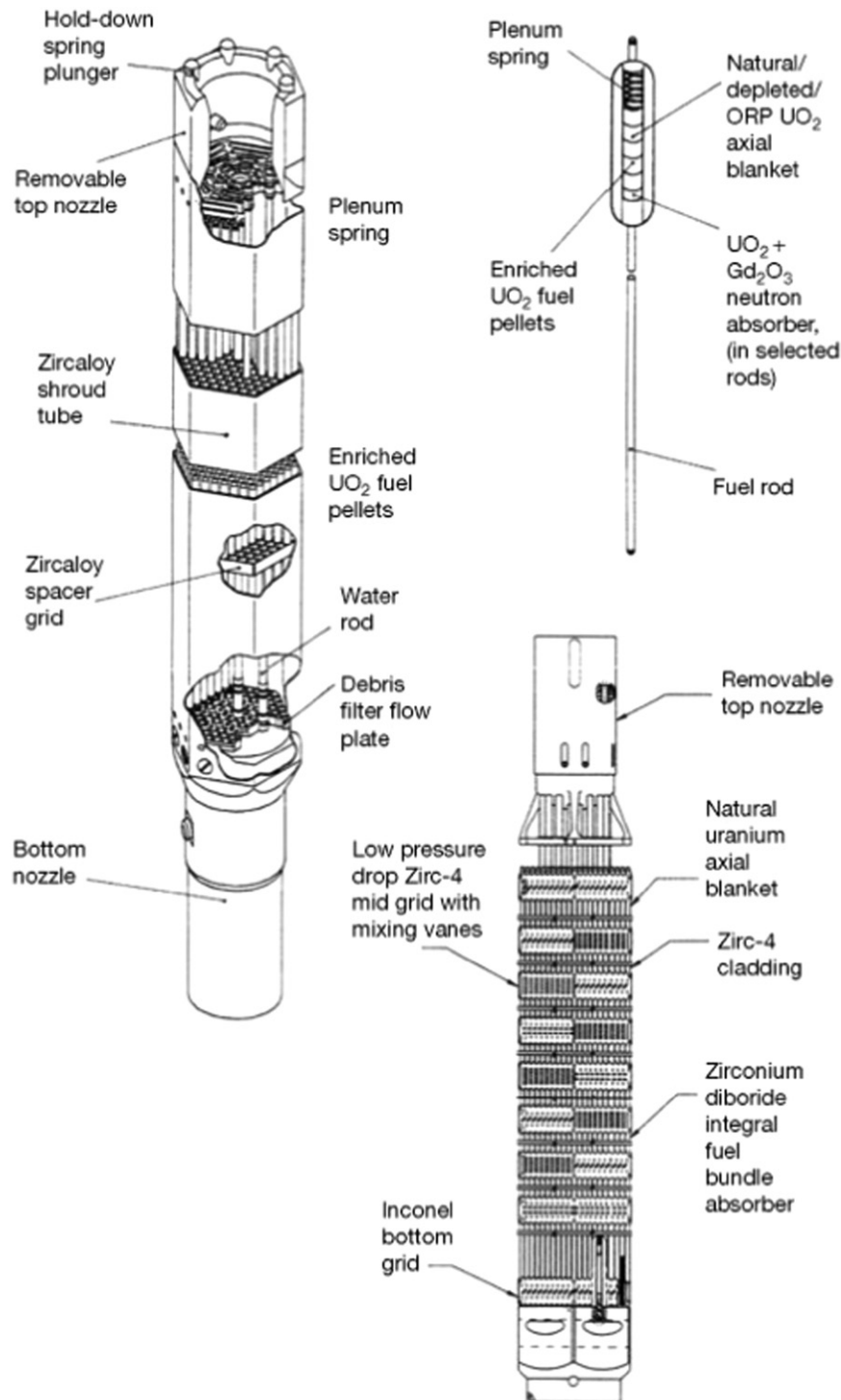
Fig. 11 Example westinghouse VVER-1000 fuel assembly. Reproduced from Tarlton, S., 2008. Nucl. Eng. Int. 53, 26–36.

2.01.3.2.5 AGR fuel

AGR fuel assemblies typically have 36 rods contained within a graphite sleeve. Twenty fuel assemblies are placed in a skip inside a flask.

2.01.3.2.6 LWR MOX fuel assembly

Plutonium recycling has so far been limited to partial loading in LWR cores. A primary design target of the MOX fuel assembly is compatibility with the UO_2 standard fuel assembly. In the neutronic design for partial loading of LWR cores, significant thermal neutron flux gradients at the interfaces between the MOX and UO_2 fuel assemblies have to be considered. The increase in thermal
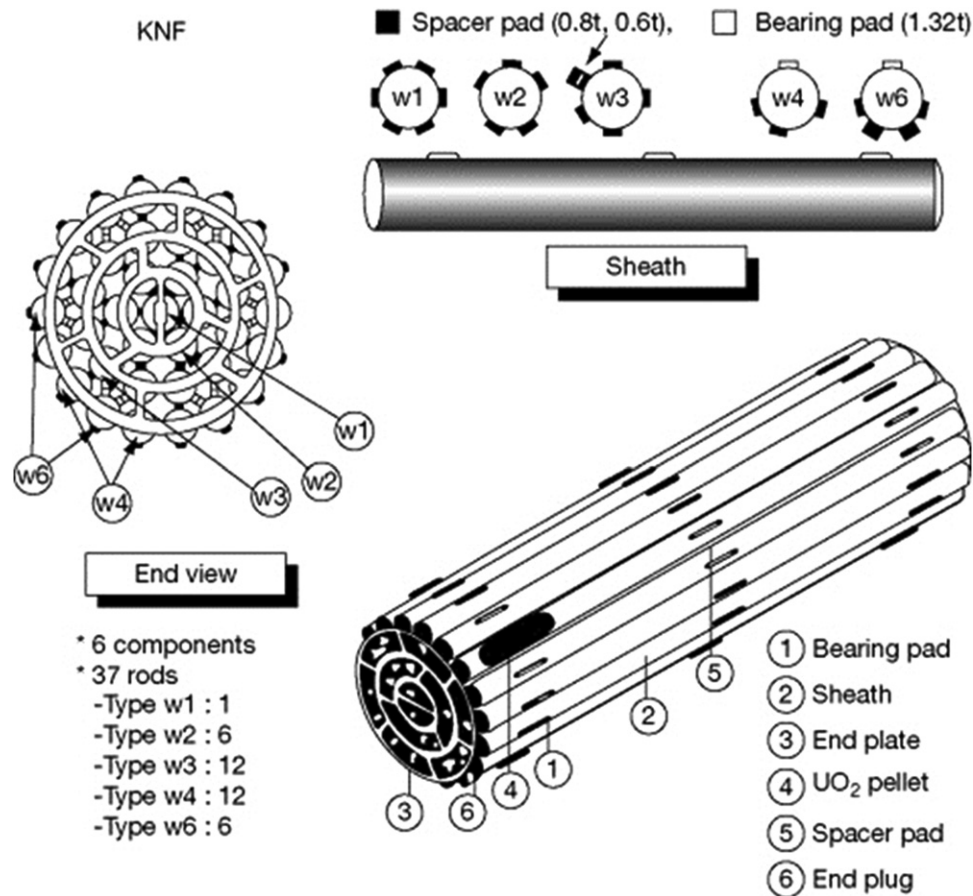
Fig. 12 Example of CANadian Deuterium Uranium (CANDU) reactor fuel assembly. Reproduced from Tarlton, S., 2008. Nucl. Eng. Int. 53, 26–36.

neutron flux in the direction of an adjacent UO_2 assembly is addressed by a gradation in the plutonium content of the MOX fuel rods at the edges and corners of the fuel assembly. There are three typical rod types for PWR MOX fuel assemblies. Optimized BWR fuel assemblies are more heterogeneous: wider water gaps and larger water structures within a BWR fuel assembly result in MOX fuel assembly designs with an increase in the number of different rod types. Examples of MOX fuel assembly designs are shown in **Fig. 13**.[2] There are plans for recycling weapons grade plutonium in PWRs in the United States.[32]

The 100% MOX cores permit an increase in the amount of plutonium under irradiation at a reduced level of heterogeneity of the core. An advanced boiling water reactor (ABWR) to be constructed in Ohma, Japan, will be the first plant with an in-built 100% MOX core capability. It is also considered to exploit the new opportunity of 100% MOX core management in the EPR.[33]

2.01.3.2.7   FBR fuel assembly

Fig. 14[2] shows an example of an FBR fuel assembly. FBR fuel assemblies have a hexagonal fuel rod arrangement with small gaps provided by a wire spacer, helically wound around each of the fuel pins or by hexagonal grid spacers. The fuel bundle is encased in a wrapper tube, in order to form a sodium flow channel for efficient cooling and to prevent fuel failure propagation during an accident.

Austenitic or ferritic steels or nickel alloys are selected as materials for structural components because of their good compatibility with sodium and their ability to cope with high temperatures and high levels of fast neutron exposure. These features of FBR fuel assembly design result from the unique design requirements of the FBRs, including the hard neutron energy spectrum, compact core size, high power density, high burn-up, high temperature, and plutonium breeding. The fuel structure and actual fuel design vary with the reactor scale, design targets, and the design methodology. **Table 3** summarizes the fuel assembly design specifications of the SUPERPHENIX, BN-600, and MONJU.[34]

2.01.4   Uranium Oxide Production

Uranium oxide has become the primary fuel for the nuclear power industry today.[35–49] As of April 2017, there are some 448 commercial nuclear power reactors operating in 30 countries, with a total capacity of 394,000 MWe.[1] Most of these reactors are of
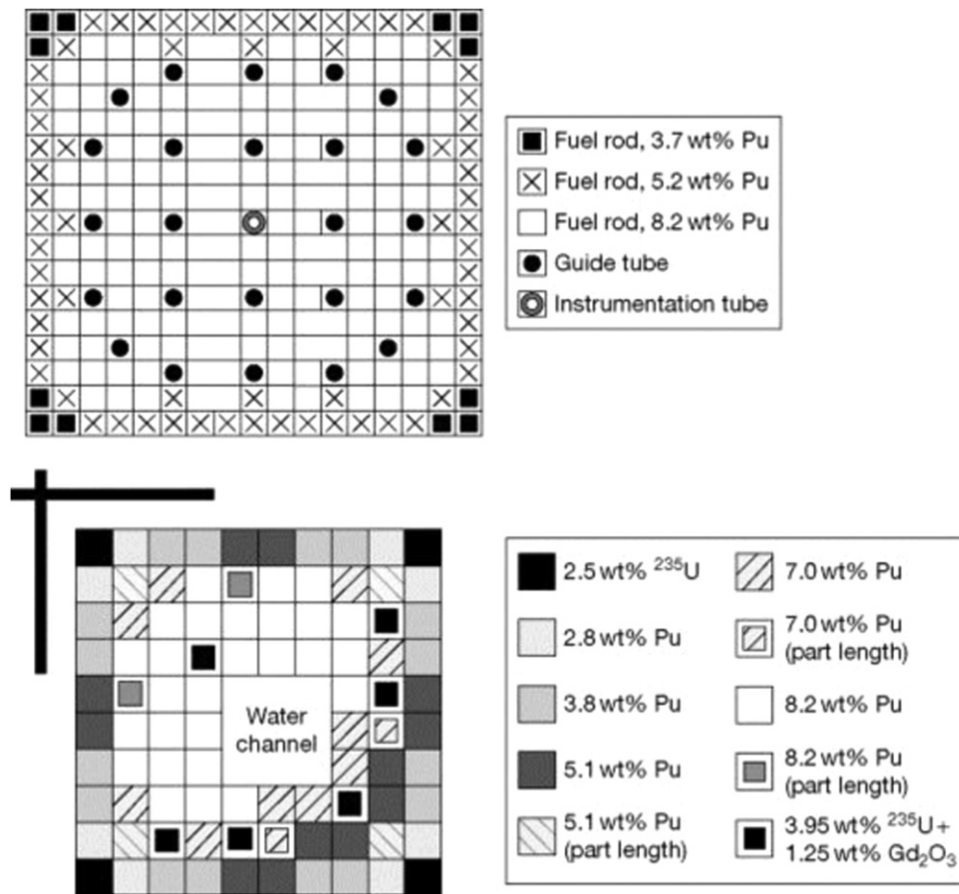
Fig. 13 Example light water reactor mixed oxide of uranium and plutonium fuel assemblies. The upper is pressurized water reactor design of the $17 \times 17 - 24$ type with a fuel assembly averaged plutonium concentration of 7.2% Pu. The lower is boiling water reactor design of the $10 \times 10 - 9Q$ type with a fuel assembly averaged plutonium concentration of 5.4 wt% Pu. Reproduced from IAEA, 2003. Status and Advances in MOX Fuel Technology. Technical Reports Series No. 415. Vienna: IAEA.

the LWRs, AGRs, or the CANDU reactor types, and they are mainly fueled with sintered pellets of UO_2 containing natural uranium or uranium enriched between 2% and 5%.

2.01.4.1   Uranium Oxide Powder Production

Prior to UO_2 pellet fabrication, the enriched uranium feed, UF_6, is converted to UO_2 powder. Although a number of conversion processes have been developed, only three are used on an industrial scale today. Two of these are wet processes: ADU and ammonium uranyl carbonate (AUC) and the third is a dry process.

The selected conversion process and its process parameters strongly influence the characteristics of UO_2 powder and the resulting UO_2 pellets.

2.01.4.1.1   ADU process

The ADU process has been widely used for many years. It uses ADU as an intermediate product in a two-step process. First, UF_6 is vaporized and injected into an ammonia solution. UF_6 hydrolyzes and precipitates as ammonium diuranate $(NH_4)_2U_2O_7$. The ADU precipitate is collected on filters and dried to get the ADU powder.

$$UF_6 + 2H_2O \rightarrow UO_2F_2 + 4HF$$
$$2UO_2F_2 + 6NH_4OH \rightarrow (NH_4)_2U_2O_7 + 4NH_4F + 3H_2O \tag{5}$$
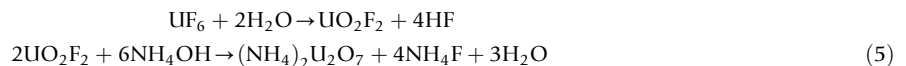
Secondly, the ADU powder is calcined and then reduced to UO_2 with hydrogen.

$$(NH_4)_2U_2O_7 + 2H_2 \rightarrow 2UO_2 + 2NH_3 + 3H_2O \tag{6}$$
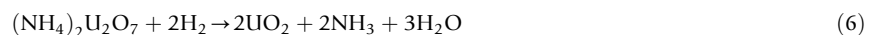
The properties of the resulting UO_2 are strongly dependent on the processing parameters of precipitation, calcinations, and reduction and equally on material contents, and reacting temperatures. For example, the amount of NH_3 is critical in the
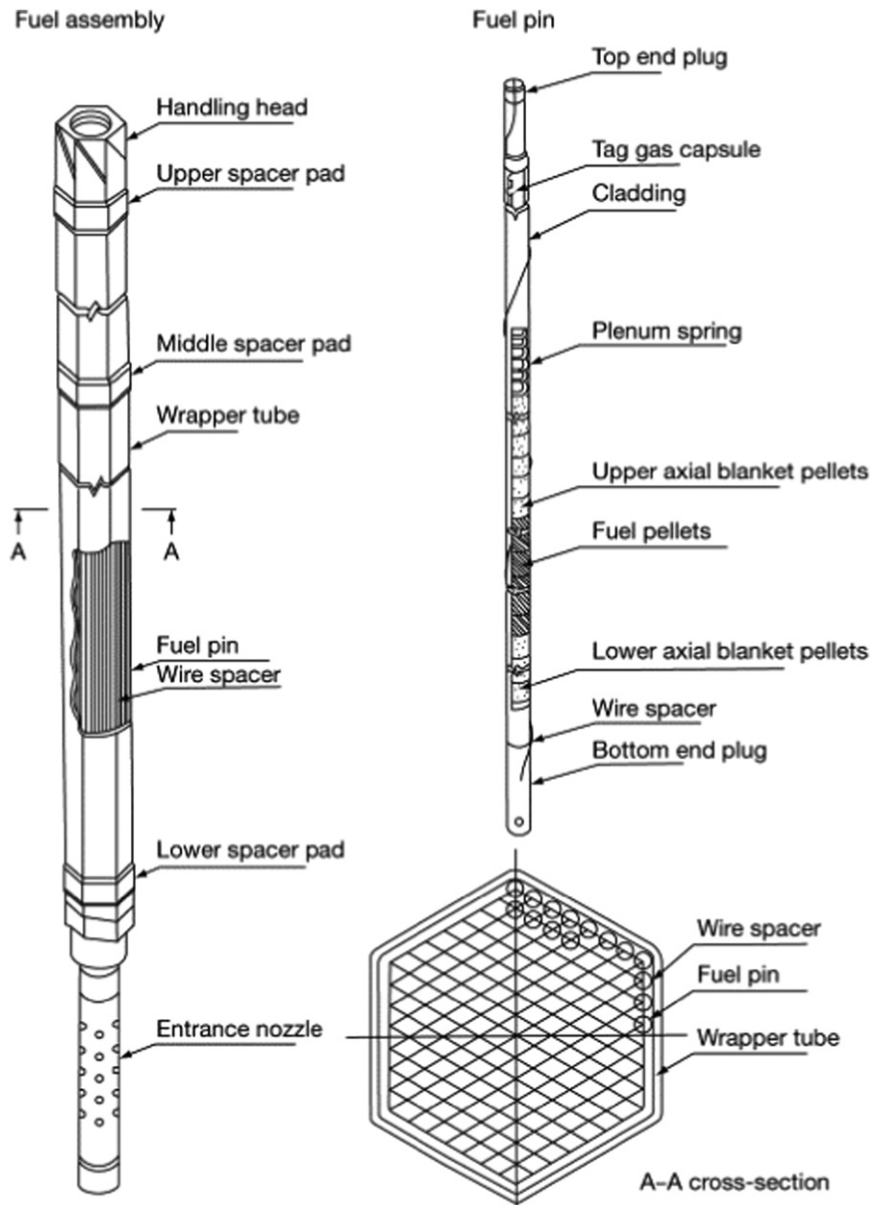
Fig. 14 Example fast breeder reactor mixed oxide of uranium and plutonium fuel assembly design of MONJU. Reproduced from IAEA, 2003. Status and Advances in MOX Fuel Technology. Technical Reports Series No. 415. Vienna: IAEA.

Table 3   Summary of fuel assembly design data of SUPERPHENIX, BN-600 and MONJU

Reactor name	SUPERPHENIX	BN-600	MONJU
No. of fuel rods per assembly	271	127	169
Assembly length (mm)	5400	3500	4200
Assembly width (mm)	173	96	110.6
Rod length (mm)	2700	2445	2813
Rod diameter (mm)	8.5	6.9	6.5
Pellet material	MOX	UO_2	MOX
Pellet diameter (OD/ID) (mm)	7.14/1.8	5.95/1.6	5.4/0
Pellet density (g cm^{-3})	95.5% TD	10.4	85% TD
Clad material	17% Cr–13% Ni stainless steel	16% Cr–15% Ni stainless steel	PNC316
Clad thickness (mm)	0.56	0.4	0.47
Average discharge burn-up (MWd kg HM^{-1})	60 (achieved)	60 (achieved)	80 (target)

Source: IAEA, 2006. Fast Reactor Database 2006 Update. IAEA-TECDOC-1531. Vienna: IAEA.

precipitation step: too much will yield gelatinous ADU which is difficult to filter; if there is too little then the resulting UO_2 powder will be inactive and difficult to press and sinter into pellets.

2.01.4.1.2   AUC process[37]

In Europe, the AUC process is widely used for fabricating UO_2 fuels. The precipitation of AUC is done in a precipitator, filled with demineralized water. The vaporized UF_6, CO_2, and NH_3 are added as gases through a nozzle system. Reaction occurs according to the following equation:

$$UF_6 + 5H_2O + 10NH_3 + 3CO_2 \rightarrow (NH_4)_4\{UO_2(CO_3)_3\} + 6NH_4F \tag{7}$$
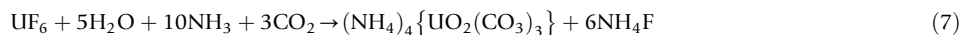
The AUC precipitates in the form of yellow single crystals. The grain size depends on the precipitation conditions. Instead of UF_6, uranyl nitrate solution can also be used as a feed material.

The AUC precipitate is filtrated and washed with a solution of ammonium carbonate and methyl alcohol. Then, the AUC powder is pneumatically transferred to a fluidized-bed furnace, decomposed, and reduced to UO_2 with hydrogen according to the following equation.
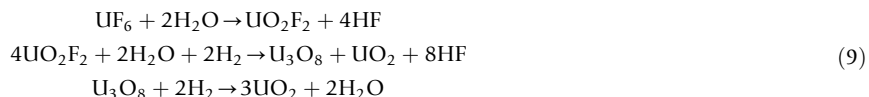
$$(NH_4)_4\{UO_2(CO_3)_3\} + H_2 \rightarrow UO_2 + 4NH_3 + 3CO_2 + 3H_2O \tag{8}$$
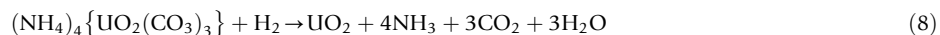
The transformation of AUC to UO_2 gives rise to desirable UO_2 powder properties: it is free-flowing and has a high sintering activity.

The resulting UO_2 powder is made chemically stable by a slight oxidation to about $UO_{2.10}$.

2.01.4.1.3   Dry process[38]

The dry process was developed in the late 1960s and is widely used today. UF_6 is vaporized from steam or hot-water-heated vaporizing baths, and vaporized UF_6 is introduced into the feed end of a rotating kiln. Here, it meets and reacts with superheated steam to give a plume of uranyl fluoride (UO_2F_2). UO_2F_2 passes down the kiln where it meets with a countercurrent flow of steam and hydrogen and is converted to UO_2 powder. The reaction sequence follows the equations below.

$$UF_6 + 2H_2O \rightarrow UO_2F_2 + 4HF$$
$$4UO_2F_2 + 2H_2O + 2H_2 \rightarrow U_3O_8 + UO_2 + 8HF \tag{9}$$
$$U_3O_8 + 2H_2 \rightarrow 3UO_2 + 2H_2O$$

The UO_2 powder resulting from dry processes is of low bulk density and fine particle size. Therefore, granulation before pressing and the employment of a pore former process are usual during the pellet fabrication process.

A dry process has preferable advantages: the process is simple and the equipment is compact; the criticality limitation is less required; and liquid waste treatment like solvent extraction is not necessary because of reaction between steam and gasses phases.

2.01.4.2   UO$_2$ Pellet Production

The flow sheet for UO_2 pellet production is shown in **Fig. 15**. The UO_2 pellet fabrication process consists of mixing the UO_2 powder with additives such as binder, lubricant and pore former materials, granulating to form free-flowing particles, compaction in an automatic press, heating to remove the additives, sintering in a controlled atmosphere, and grinding to a final diameter. The process varies slightly according to the nature of the starting UO_2 powder.

2.01.4.2.1   Powder preparation

In the pelletizing process, UO_2 powder must be filled easily and consistently into dies. UO_2 powder from the AUC process is free-flowing and can be pressed without granulation. Usually it is mixed with a small amount of U_3O_8 to control the density and pore distribution of the pellets. The fine particle size of the integrated dry route (IDR) powders prevents them from being free-flowing when produced; these powders are therefore prepressed into briquettes, fractured, sieved to produce granules, and a dry lubricant added. ADU powder is slurried with a solvent and a volatile binder such as polyethylene glycol or polyvinyl alcohol, spray dried and sieved to size. The obtained material flows freely and will consistently fill pellet dies but an extra operation is required to remove the binder. Additives known as pore formers are often included to give a uniform final density: 95%–97% TD for LWR UO_2 and MOX, and 85%–95% TD for FBR MOX fuel pellets. The pore former will decompose in the dewaxing process to leave closed pores that are stable in-reactor.

2.01.4.2.2   Pelletizing

The prepared UO_2 powder is pressed into green pellets in reciprocal or rotary presses at 150–500 MPa. The density of green pellets reaches 50%–60% TD. Pellets are normally fabricated with dished ends and/or chamfered edges. The dishes compensate for radial variation in thermal expansion in-reactor, and the chamfers reduce the pellet–cladding mechanical interaction (PCMI). In VVERs and some fast reactors, pellets are made with a central hole to reduce fuel centerline temperatures. The pressing actions of the dies and the punches are carefully controlled to obtain a homogeneous local density distribution in the green pellet and to prevent defects in the green pellet. Two typical LWR UO_2 pellets are shown in **Fig. 16**.
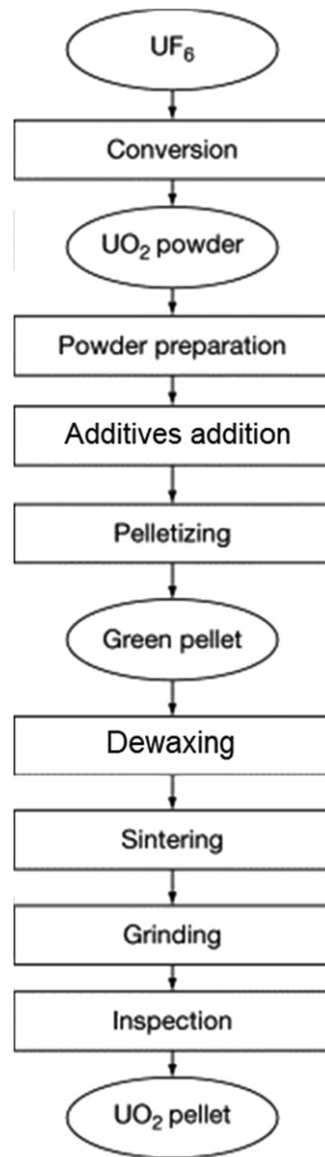
Fig. 15 Flow sheet for UO$_2$ pellet production.
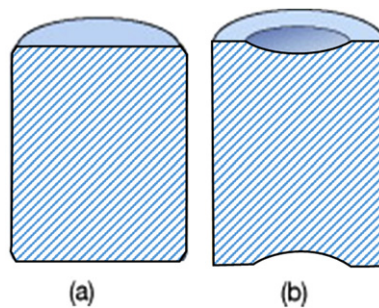

Fig. 16 Typical light water reactor UO$_2$ pellets. Pellet with (a) chamfer and (b) dish.

2.01.4.2.3 Dewaxing and sintering

The volatile additives such as binders, lubricants and pore formers (if used) are removed from the green pellets by heating at 600–800°C in a furnace for several hours. The additives will decompose into harmless gases at low temperature. This dewaxing

process is generally done as the first step of the sintering process. The green pellets are then sintered in hydrogen gas flow to adjust O/U to 2.00 at 1600–1800°C for times that are based on control samples from previous batches, but are typically 3–10 h. U_3O_8 powder, mixed with the original UO_2 powder, can also be used to control the final product density.[39]

The properties of UO_2 fuel pellets such as thermal conductivity, gas bubble mobility, and creep rate, influence fuel performance in-reactor. These properties are affected by the grain size and the porosity distribution of the pellets. Early LWR fuel pellets had a small grain size (2–3 μm), but the requirement for greater fission gas retention by large grain fuel has led to the current use of 10–20 μm grain size material. As higher burn-ups become required, greater fission gas retention in the fuel pellets may be expected in the future. The grain size of UO_2 pellets can be increased by controlling the sintering conditions or by using sintering additives such as Al_2O_3, SiO_2, TiO_2, Nb_2O_5, or Cr_2O_3.[40–42]

2.01.4.2.4 *Finishing and inspecting*

As-sintered pellets have an hour-glass shape because of the internal density distribution generated during pressing, and the diameter of the pellet must be accurate at 10 μm, also, from the viewpoint of gap conductance, the pellet surface must be smooth. Therefore, pellets are ground by a centerless grinding machine.

After grinding, each pellets are inspected to check their diameter, length, density, and appearance; inspections are almost completely automated except for appearance. Analyses for their uranium enrichment, impurities, and microstructures are also done on randomly selected pellets within each batch.

2.01.4.3 Burnable Poison-Doped Fuel Production[43]

The fabrication process of the gadolinium-doped fuel is almost the same as that of the UO_2 fuel. The gadolinium-doped fuel fabrication line must be separated from the UO_2 fuel to prevent gadolinium from contaminating the UO_2 fuel fabrication line. Gadolinia is added in UO_2 by ball milling process in the powdering step, or by coprecipitation process and heat treatments.

2.01.5   MOX Production

The utilization of plutonium in reactors is essential for the establishment of the nuclear fuel cycle. It is already being used in LWRs and research and development (R&D) has been continued to utilize plutonium more efficiently in FBRs. MOX fuel is often selected as FBR fuel because of its excellent burn-up potential, high melting point, and relative ease of commercial fabrication and also because LWR fuel fabricators already have extensive experience with UO_2 fuel fabrication. Furthermore, oxide fuel has good irradiation stability, and proven safety response using a negative Doppler coefficient that mitigates over-power transients.[42,43] These advantages must be weighed against the disadvantages of oxide fuel, such as lower thermal conductivity that leads to fuel temperature increase,[44] reduced compatibility with sodium,[45–47] low fissile atom density, and the presence of two moderating atoms per one metal atom. Based on a balance between the advantages and disadvantages, various fabrication processes for MOX fuels, including the conversion processes for plutonium oxide, were developed more than 40 years ago and are still applied. Major processes utilized in the conversion of plutonium oxide and MOX fuel production are summarized here. Their details have been described in the literature.[2,9,27,29,42,48]

Plutonium emits α-particles with energies higher than 5 MeV, and all operations, from powder handling to end plug welding after pellets are loaded into a cladding tube, are carried out in glove boxes. In order to prevent plutonium inhalation accidents during fuel fabrication, these glove boxes have an airtight structure and their interiors are continuously kept at negative pressure. Furthermore, as described in Section 2.01.2.8, gamma and neutron shielding is required for these glove boxes to reduce radiation exposure.[49]

2.01.5.1   Plutonium Powder Production

Plutonium is extracted from spent fuels in the reprocessing plants in the form of plutonium nitrate. In order to utilize extracted plutonium for MOX fuel production, plutonium nitrate is converted to oxide powder by three methods: one is an oxalate precipitation method; the other two methods involve coconversion with uranium, the ammonium uranyl plutonyl carbonate (AUPuC) conversion method, and the microwave heating denitration method (MH method). The AUPuC conversion method is described in Section 2.01.5.2.3 as part of the AUPuC fuel fabrication process.

2.01.5.1.1   *Oxalate precipitation method*

In the oxalate precipitation method, the plutonium oxide powder is prepared from plutonium nitrate by the following two reactions.[50]

$$Pu(NO_3)_4 + 2(COOH)_2 \rightarrow Pu(COO)_4 + 4HNO_3$$

$$Pu(COO)_4 \rightarrow PuO_2 + 2CO_2 + 2CO \tag{10}$$
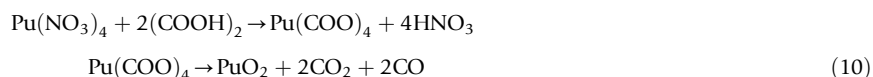
Oxalate acid, $H_2(COOH)_2$, is added to plutonium nitrate solution at about 60°C, and the temperature maintained until the precipitation reaction (1) is completed. The plutonium oxalate precipitate is filtered and then dried in air. Dried plutonium oxalate

is calcined in a furnace at temperatures from 350 to 650°C. It has been reported that reaction (2) begins below 100°C and is completed at around 350°C.[50] The characteristics of the obtained PuO$_2$ powder vary depending upon the precipitation and calcination conditions, that is, the precipitation temperature, addition rate of oxalate acid to plutonium nitrate, oxalate acid concentration, and calcination temperature. This PuO$_2$ powder is commonly utilized as a feed material for MOX fuel production in the world. The microstructure and characteristics of PuO$_2$ powder prepared by the oxalate precipitation method have also been explained elsewhere.[8]

2.01.5.1.2 Microwave heating denitration method

To increase the proliferation resistance of plutonium, a coconversion method of adding plutonium nitrate and uranyl nitrate to a mixed oxide powder was developed in Japan. In the MH method, about 7 l of a mixed solution of uranyl nitrate and plutonium nitrate with a concentration of about 250 g l^{-1} of heavy metal, is fed into a denitration vessel. The diameter and height of this silicon nitride vessel are about 50 and 6 cm, respectively. After microwave irradiation (2450 MHz, 16 kW), PuO$_2$ + UO$_3$ is formed, and then this product is calcined to PuO$_2$ + U$_4$O$_9$ + U$_3$O$_{\overline{8}x}$ in air for 2 h at 750°C. Subsequently, this mixture is reduced to PuO$_2$ + UO$_2$ (MH-MOX) powder under an atmosphere of N$_2$–5% H$_2$ mixed gas, at the same temperature used for calcination.[13] The obtained MH-MOX powder has sufficiently good powder characteristics to allow fabrication of MOX pellets of more than 95% TD.[13,51] Full details of the MH method have been given elsewhere.[51–54] With the MH method, the generation of radioactive liquid waste containing plutonium is reduced compared with other conversion processes.

Fig. 17 shows microstructures which were observed by scanning electron microscopy (SEM) at 10,000-fold magnification, in the PuO$_2$ powder (A) prepared by the oxalate precipitation method and MH-MOX powder (B). The microstructures of MH-MOX powder and UO$_2$ powder (prepared by the ADU process) calcined at various temperatures have been reported in Asakura *et al.*[13]

Examples of the characteristics of PuO$_2$ and MH-MOX powders are shown in Table 4. The values vary depending on the conversion conditions described above.

2.01.5.2 MOX Pellet Production

In the beginning stages of R&D for MOX fuel production, many kinds of manufacturing techniques were investigated. In the 1960s, the pellet route was adopted for all the pilot plants in Belgium, France, Germany, the United Kingdom, and Japan.[2,48] The two types of MOX fuel for LWRs and FBRs have quite different characteristics, affecting both the fabrication process and the quality requirements. These characteristics are summarized in the following points[9]:

(1) The plutonium content of FBR fuel is several times higher than that of LWR fuel.
(2) The smear density of FBR fuel has to be lower than that of LWR fuel because the former has to be used at higher temperature and for higher burn-up.
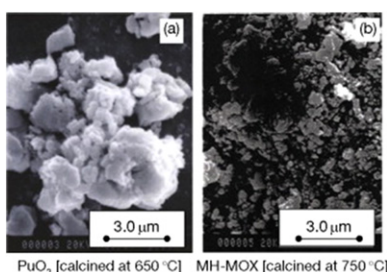

PuO$_2$ [calcined at 650 °C]   MH-MOX [calcined at 750 °C]

Fig. 17 Microstructures of PuO$_2$ and MH-MOX powders observed by scanning electron microscope.

Table 4 Characteristics of PuO$_2$ and MH-MOX powders

	PuO$_2$ powder prepared by the oxalate precipitation method	MH-MOX powder prepared by the microwave heating denitration method
Calcination temperature and atmosphere	650°C in air	750°C in air
Reduction temperature and atmosphere	–	750°C in N$_2$ + 5% H$_2$
BET specific surface area (m^2 g^{-1})	15.35	3.70
Average particle size (μm)	4.60	4.28
Bulk density (g cm^{-2})	2.66	2.20
Tap density (g cm^{-2})	3.56	3.40

(3) The higher plasticity of FBR fuel, resulting from the higher irradiation temperature, justifies less restrictive specification tolerances and quality requirements, than for LWR fuel.

(4) The uniformity of Pu isotopic composition within a batch of FAs is a key performance related quality for LWR fuel (Pu 239 and Pu 241 being fissile, both with quite different reactivity values, and Pu 240 and Am 241 being neutron absorbers), while it is rather unimportant for FBR fuel (all the Pu and Am isotopes being fissile to some degree);

On the basis of these points, various kinds of processes were developed to fabricate MOX pellets for FBRs and LWRs. The MOX pellet fabrication processes that have been adopted in several countries are described below.

2.01.5.2.1   *Belgium*

In Belgium, the micronized master blend (MIMAS) process was developed by Belgonucléaire (BN) in the early 1980s based on the experiences acquired in the reference fabrication process developed earlier and commercially used in the 1970s at BN's Dessel plant.[2] The reference process consisted of a single blending of PuO_2 powder with free-flowing UO_2 powder and this blending resulted in a blend with adequate flowability to feed the pelletizing press.[9] As MOX pellets fabricated by the reference process could not satisfy the preprocessor's new requirement, which was that MOX pellets had to be soluble in a nitric acid solution, BN had to improve the solubility of MOX pellets in the nitric acid solution due to the poor solubility of $(U,Pu)O_2$ with a high Pu concentration. In order to improve their solubility, the MIMAS process was introduced in the Dessel plant. **Fig. 18** shows the flow sheet for the MIMAS process.

In the MIMAS process, suitable amounts of PuO_2 powder, UO_2 powder, and dry recycled scrap powder are prepared to get a 60 kg MOX master blend powder with 30% plutonium concentration. The master blend powder is ball milled to obtain a homogeneous distribution of plutonium. In the second blending, force-sieved (i.e., micronized) master blend powder is diluted with the free-flowing UO_2 powder and additional dry recycled scrap to form 80 kg of the final blended MOX powder with the desired plutonium concentration.[9] In this step, it is very important to obtain uniform distribution of master blend in free-flowing UO_2 powder. This final blended MOX powder is pelletized into green pellets using a pressing machine with multiple punches and a reciprocating mechanism. Approximately 10–12 green pellets can be pressed simultaneously. These green pellets are sintered at about 1700°C under a reduced atmosphere of Ar + H_2 mixed gas, after dewaxing. Not only does the intimate contact between the co-micronized UO_2 and PuO_2 powders provide adequate interdiffusion during sintering and therefore enhanced solubility, but also the larger contact area between the more abundant fine powder and the free-flowing UO_2 powder results in a more homogeneous MOX structure than in the earlier reference process. This is apparent in measurements such as the α-autoradiograph of a transverse section of a MOX pellet prepared by the MIMAS process.[55,56]
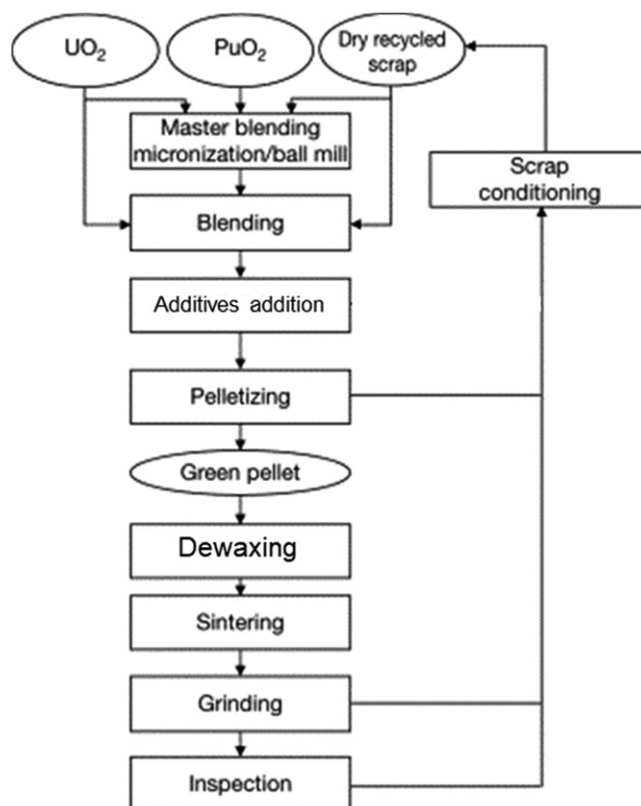

Fig. 18   Flow sheet for the micronized master blend process.

During the 1990s, the Dessel plant accounted for over 60% of the world's production of MOX fuel.[49] However, MOX fuel fabrication was terminated in 2006. The main decommissioning including the dismantling of glove boxes was carried out in the period from 2010 to 2013.

2.01.5.2.2 France

In France, the Complexe de Fabrication de Cadarache (CFCa) started operation in 1962, on a pilot scale, for developing FBR fuel. The Cobroyage (co-milling) Cadarache (COCA) process was developed there in the 1970s to fabricate MOX pellets for FBRs using two fuel fabrication lines.

Fig. 19 shows the flow sheet for the COCA process. It utilizes an optimized ball mill as a blender and involves the forced extraction of the lubricated micronized powder through a sieve. This results in free-flowing granules which are suitable for feeding at the pelletizing step.[48] In the COCA process, the lubricant and the porogen, which is a pore former to control pellet density, are added to the force-sieved powder.[8] One of the two FBR fuel fabrication lines in CFCa was switched to a LWR MOX fuel fabrication line which introduced the LWR fuel fabrication technology developed by BN. This LWR fuel fabrication line started producing PWR fuel in 1990.[9] MOX fabrication at CFCa was stopped in 2005 because of seismic safety issues and the facility is now undergoing decommissioning.

In 1985, the construction of the MELOX plant at Marcoule was started; it had an annual production capability of 100 tons of heavy metal (tHM) for PWR fuel which was decided on the basis of operational experiences with the MIMAS process obtained at CFCa and it started MOX fuel production in 1995. Gradually, its licensed annual production capability was expanded and it
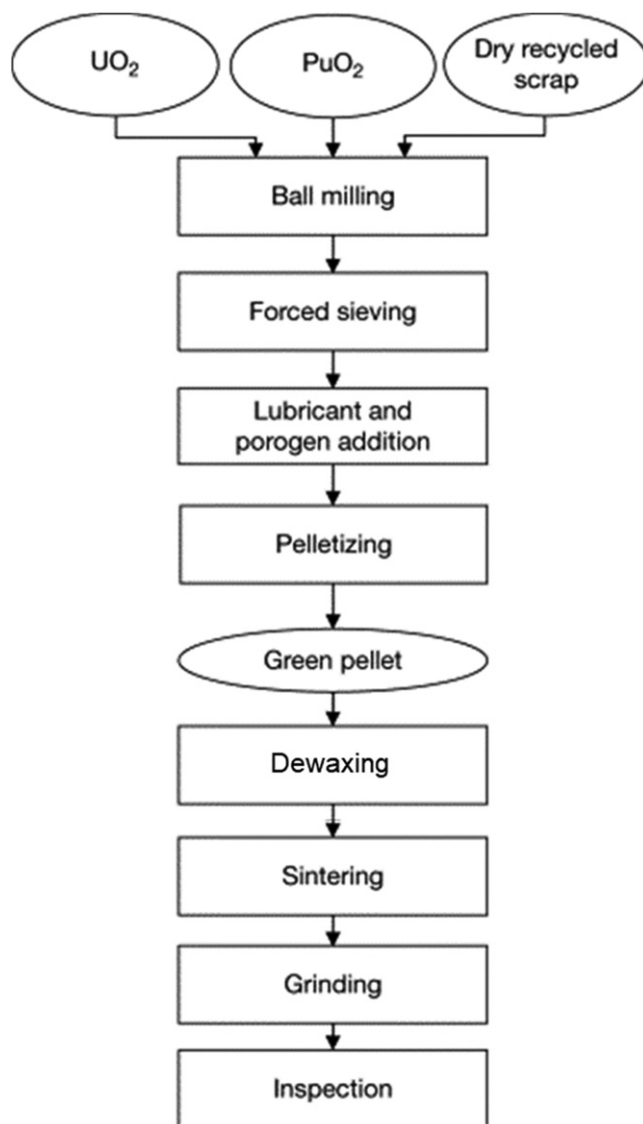

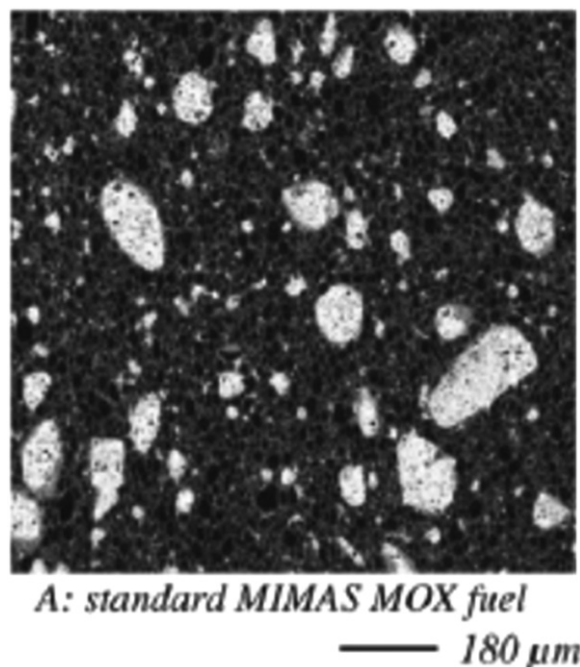**Fig. 19** Flow sheet for the cobroyage (co-milling) cadarache process.

Fig. 20   X-ray images of Pu in standard MIMAS MOX pellet. Reproduced from Oudinet, G., Munuz-Viallard, I., Aufore, L., *et al.*, 2007. J. Nucl. Mater. 375, 86–94.

reached 195 tHM as of April 2007; MOX fuel fabrication for BWRs was also covered during this expansion. The process adopted in the MELOX plant is called the advanced MIMAS process and its flow sheet is shown in **Fig. 21**. The accumulated MOX fuel production at the MELOX plant reached more than 2600 tHM. The features of this process are given below.

In order to utilize up to 50% of dry recycled scrap powder in the master blend powder and to achieve excellent homogeneity and uniformity of PuO_2 as well, a new ball mill was developed for the first blending step.[9] This mill uses three-dimensional movement and U–Ti alloy balls. For the second blending, a high capacity (640 kg) blender consisting of a conical screw mixer with a double envelope cooling system was adopted.[9,49] In order to achieve MOX fuel production on a large scale, complete automation was implemented in the production line. Similar to the original MIMAS process invented in BN, three kinds of feed powders, PuO_2 powder, UO_2 powder, and dry recycled scrap powder, are ball milled to obtain the master blend powder with about 30% plutonium concentration. The force-sieved master blend powder is diluted with the free-flowing UO_2 powder, prepared by the ADU process or the AUC process and additional dry recycled scrap powder using the high capacity conical screw mixer. This free-flowing diluted power is pelletized into green pellets using a pressing machine with multiple punches and a reciprocating mechanism. Approximately 10–14 green pellets can be pressed simultaneously. The green pellets are sintered in a continuous-type sintering furnace consisting of a dewaxing part and a sintering part. After dry centerless grinding of sintered pellets, the exterior of all pellets are inspected.

A mapping image of plutonium, acquired by X-ray microanalysis of a transverse section of a MOX pellet prepared by the advanced MIMAS process, was reported in previous works.[55–57] An X-ray image of Pu in the MIMAS MOX is given in **Fig. 20**.[56] White Pu rich phase of 10–200 μm is observed in the MIMAS pellet. In the MIMAS process, a two-step blending method is utilized to obtain the desired plutonium content in the pellets, as described above. This results in the presence of two or three phases in the transverse section of a sintered pellet. The MOX pellets prepared with UO_2 powder from the ADU process show three phases, plutonium rich clusters, a coating phase and a UO_2 phase on their transverse sections while those prepared with UO_2 powder from the AUC process show two phases, plutonium rich clusters and a UO_2 phase.[55,57] The MOX pellets currently manufactured in the MELOX plant are reported to have a mean grain size of 5.8 μm.[58]

2.01.5.2.3   Germany

Two MOX pellet fabrication processes were developed in Germany, the Optimized CO-Milling (OCOM) process and the AUPuC process.[10,58]

The OCOM process was developed by Alkem and uses UO_2 powder, PuO_2 powder, and recycled scrap powder as feed materials. The manufactured MOX pellets are made fully soluble in nitric acid by optimizing the co-milling of the three powders. In the OCOM process, two different MOX pellet fabrication routes can be taken as shown in **Fig. 22**.

In the first route (left half of **Fig. 22**), three powders are prepared to achieve specified plutonium concentrations required for the fuel to be used in FBRs and LWRs. The powders are co-milled to obtain a homogeneous distribution of plutonium, and the milled powder is pressed into green pellets after granulation. The second route (right half of **Fig. 22**) is used to fabricate MOX pellets for
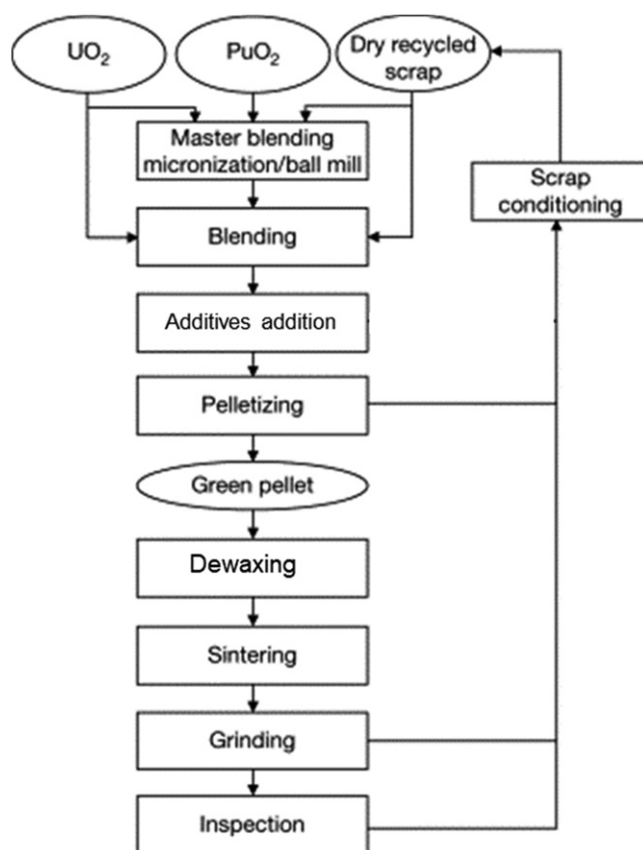
Fig. 21 Flow sheet for the advanced micronized master blend process.

LWRs; it effectively introduces the master blend concept into the process for better economy.[10] This means that a mixture containing $\sim 30\%$ plutonium is made from UO_2 powder and PuO_2 powder, and this mixture is then milled using the OCOM milling process. The MOX powder that results from the milling process is no longer free-flowing. By mixing this master blend with the eight- to tenfold amount of free-flowing UO_2 powder to obtain the required plutonium content for LWR MOX fuel, a feed powder is obtained with sufficient flowability for direct pelletizing. An issue requiring special attention for this route is the homogeneity of the plutonium distribution; two powders of very different physical properties have to be mixed together to obtain the desired plutonium content. One powder is the master blend of PuO_2 and UO_2, which, after milling, consists of a powder with very fine non-flowing grains and having a high tendency to self-agglomerate, while the second part is the free-flowing UO_2 powder prepared by the AUC process with its rather coarse grains.[10] The mixing of the two powder components and preventing their segregation during further processing steps require special attention and expertize. The green pellets prepared by the two routes are sintered in a reducing atmosphere after dewaxing. A typical α-autoradiograph of a transverse section of a LWR pellet manufactured by the OCOM process has been reported by Roepennack et al.[58] The density and appearance of sintered pellets are inspected after centerless grinding.

The AUPuC process (**Fig. 23**[10]) was developed as a coprecipitation process based on the AUC process. The AUPuC process uses plutonium in the form of a nitrate solution. NH_3 and CO_2 gases are introduced into a mixed solution of plutonium nitrate and uranyl nitrate with a concentration of about 400 g l^{-1} of heavy metal at first, and then tetra-ammonium tricarbonate dioxo urinate/plutonate is precipitated by the following reaction.[10]

$$(U, Pu)O_2(NO_3)_2 + 6NH_3 + 3CO_2 + 3H_2O \rightarrow (NH_4)_4\left[(U, Pu)O_2(CO_3)_3\right] + NH_4NO_3 \qquad (11)$$
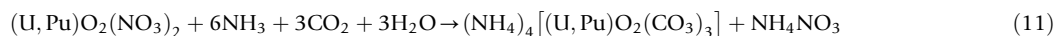
The precipitated AUPuC is filtered and directly reduced at $\sim 750\,^\circ C$ in an atmosphere of hydrogen gas. The obtained MOX powder with about 30% plutonium concentration is utilized as the master blend and is the same as in the OCOM process. The homogeneity of plutonium in the master blend is much better in the AUPuC process than in the OCOM process because solid solutions have already formed during precipitation in the AUPuC process. This coconverted powder is also diluted like the master blend by the free-flowing UO_2 prepared by the AUC process and recycled MOX powder so that the final blended MOX powder has the desired plutonium concentration. This final blended MOX powder flows easily, just as in the OCOM process, and it is pressed into green pellets by a rotary pressing machine without granulation.[42] The steps after pelletizing are the same as those in the
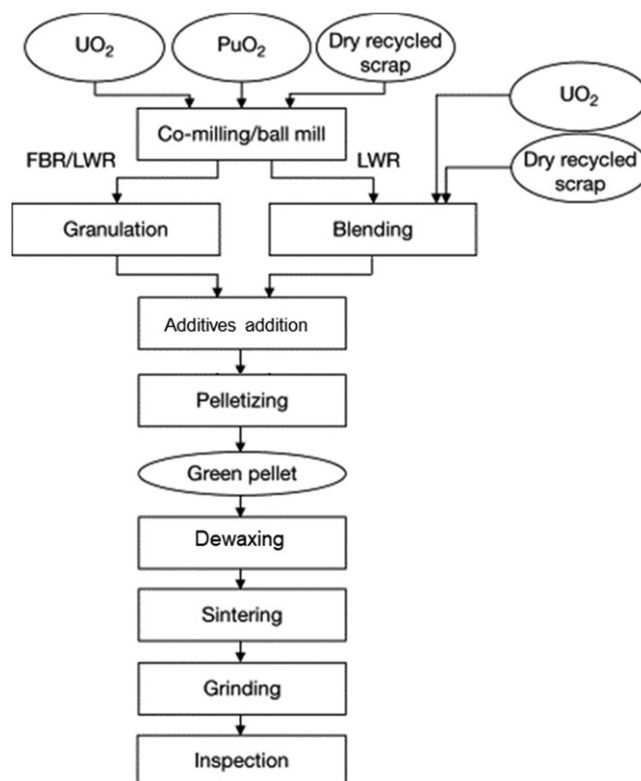
Fig. 22 Flow sheet for the optimized co-milling process.

OCOM process. A typical α-autoradiograph of a transverse section of a LWR pellet manufactured by the AUPuC process has also been reported by Krellmann.[10]

On the basis of the above processes, Siemens constructed the MOX fuel fabrication facility in Hanau as a dual purpose (FBR and LWR) facility and started operation in 1972. After reaching an effective capacity of 20–25 tHM per year of LWR fuel in the 1987–1991 period, it was shut down, as a result of a contamination incident in 1991.[9] This plant was subsequently decommissioned. On the same site, Siemens constructed a larger plant with an annual capacity of 120 tHM for LWRs.[10] However, this plant was abandoned before starting operation because Siemens never received an operating license from the local government.

2.01.5.2.4 Japan

Early in the 1960s, comprehensive R&D programs concerning MOX fuel were started in Japan and they resulted in the JAEA process that was adopted by the Plutonium Fuel Fabrication Facility (PFFF) which started operation in 1972. The PFFF used local control equipment to fabricate MOX fuel for the advanced thermal reactor FUGEN,[59] and the experimental fast reactor JOYO on an engineering scale. Following the completion of the Plutonium Fuel Production Facility (PFPF) in 1987, MOX fuel fabrications for JOYO and the prototype FBR MONJU have been conducted in PFPF since 1988. MOX fuel fabrication for FUGEN in PFFF was completed in 2001. In 2019, this plant is undergoing decommissioning.

Fig. 24 shows the flow sheet of the JAEA process utilized in the PFPF. Two kinds of plutonium, either PuO_2 powder prepared by the oxalate precipitation or the MH-MOX powder, can be used in the JAEA process to fabricate FBR MOX pellets.

In this process, three feed powders, UO_2 prepared by the ADU process, PuO_2 or MH-MOX powder, and dry recycled scrap powder, are prepared to get the plutonium concentration specified by the fuel specifications in the mixed powder. The feed powders are ball milled to get a homogeneous distribution of plutonium in the sintered MOX pellets. This mill pot has a silicon rubber lining on its inner surface to enhance the charging and discharging of powders by automated operation. About 40 kg of powder can be charged in this ball mill. A photograph of the ball mill is shown in **Fig. 25**.

Similar to the milled powder in the SBR process (see Section 2.01.5.2.5), this powder must be granulated to provide a free-flowing property.[8,13] After mixing zinc stearate (binder) and Avicel (microcrystal cellulose; pore former) with the milled powder, this powder mixture is roughly pressed into tablets at pressures of around 200 MPa and the tablets are then crushed into granules of sizes that make them free-flowing. These granules are pelletized into green pellets at pressures of around 500 MPa followed by the addition of zinc stearate as lubricant. Normally, these green pellets are sintered at about 1700°C for 4 h under an atmosphere of Ar + 5% H_2 mixed gas after dewaxing at about 800°C for 2 h under the same atmosphere as used in the sintering.[60] A ceramograph of a transverse section of a sintered MOX pellet prepared by the JAEA process is shown in **Fig. 26**. This MOX pellet was fabricated under specifications for pellets to be loaded in the MONJU outer core. The MOX pellets manufactured by Japan
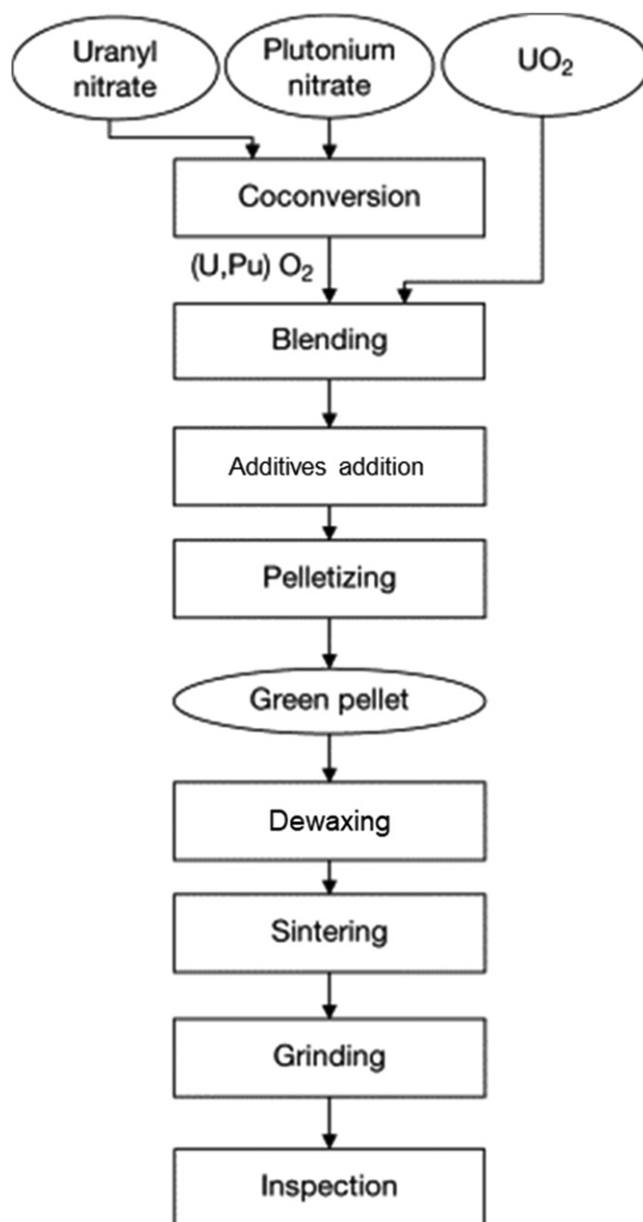
Fig. 23 Flow sheet for the ammonium uranyl plutonyl carbonate process.

Atomic Energy Agency (JAEA) processes in which a one-step blending method is adopted to obtain the desired plutonium concentration of pellets show a single homogeneous phase on their transverse sections. **Fig. 27** shows Pu distribution in the MOX pellet prepared by JAEA method which were observed by α-autoradiography and EPMA, and the pellet is homogeneous.

After centerless grinding, the diameter, geometrical density, and appearance of each sintered pellet are inspected. An inspection device to check pellet density and appearance is shown in **Fig. 28**; it is installed in the PFPF. Details of the JAEA process and its fuel fabrication technologies have been previously reported in the literature.[60,61]

2.01.5.2.5 United Kingdom

In the United Kingdom, extensive work has been carried out on the manufacture of MOX fuel under the support of the UK Fast Reactor Development Program.[8]

Based on these experiences, the SBR process was developed by the British Nuclear Fuels plc (BNFL) to fabricate MOX pellets for LWRs. The process was originally developed in the 1980s by BNFL-UKAEA (United Kingdom Atomic Energy Authority). However, the MOX fuel plant at Sellafield was closed in 2011.

Fig. 29 shows the flow sheet for the SBR process. In the SBR process, three kinds of feed materials, PuO_2 powder prepared by the oxalate precipitation method, UO_2 powder prepared by the ADU process, and dry recycled scrap powder are prepared to get the
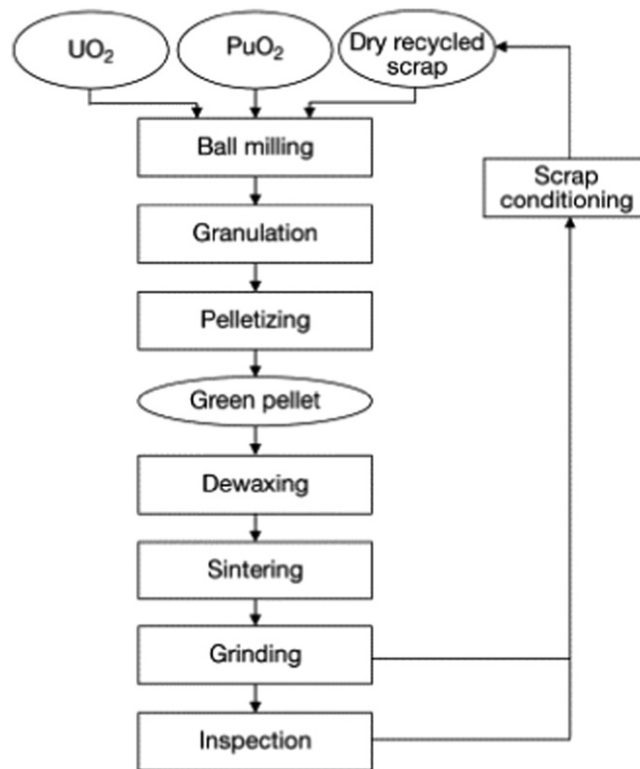
Fig. 24   Flow sheet for the Japan Atomic Energy Agency process.

Fig. 25   The ball mill used in the plutonium fuel production facility.

desired plutonium concentration in the initially mixed powder. These powders are milled completely using an attritor mill (a photograph is shown in MacLeod and Yates[8]), an off-the-shelf mill widely used in the pharmaceutical industry. The attritor mill provides good blends with a homogenized plutonium distribution in a short blending time and can be operated continuously.[9] The milled MOX powder must be granulated in order to provide a free-flowing, dust-free feed to the pelletizing press to ensure uniform die filling and good compaction.[8] In the milling step, the lubricant and Compo pore former are added in order to control the pellet density and obtain characteristics similar to those of the UO_2 pellets produced by BNFL from IDR UO_2 powder.[61] In order to condition the milled MOX powder to form granules prior to pelletizing and sintering, a spheroidizer is introduced instead of the precompaction granulation equipment commonly used.[9] The spheroidizer is used in a powder agglomeration process and was invented by SCK·CEN (Belgian Nuclear Research Center) in the 1970s to fabricate a fuel kernel, the pit of coated particles fueling high temperature reactors.[9]

In the SBR process, the binder that is commonly used in the conventional MOX fuel manufacturing process is not used. As a result, the dewaxing step of the green pellets prior to sintering is not needed and the process is similar to the current UO_2 fuel
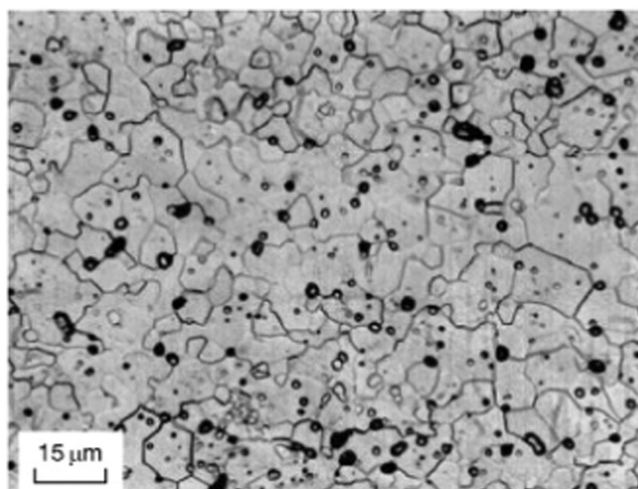
Fig. 26 Ceramograph of a transverse section of a sintered mixed oxide of uranium and plutonium pellet for MONJU fuel prepared by the Japan Atomic Energy Agency process (plutonium content: 30.8 wt%, density: 84.84% theoretical density, mean grain size: 3.9 μm).
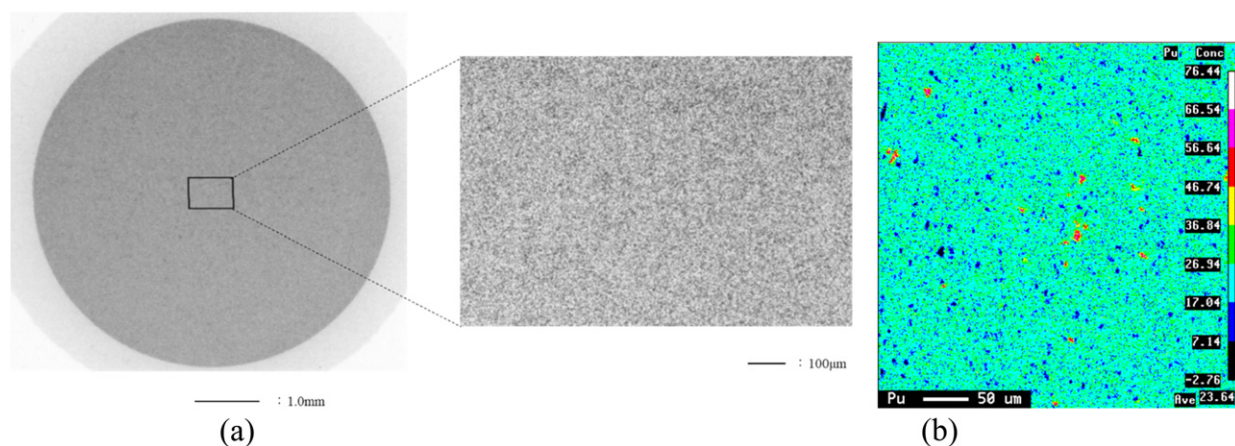

Fig. 27 Homogeneity of a JAEA MOX pellet, (a) α-autoradiograph, (b) X-ray image of Pu distribution.

fabrication process in this respect. The processing time is short and the equipment can be stacked so that the powder can be discharged by gravity from the feed dispensing and dosing glove box through the processing equipment into the hopper of the pelletizing press. The simple sequence of one attritor mill and one spheroidizer, utilized in the Manufacturing Demonstration Facility, was made more sophisticated for the Sellafield MOX Plant by the addition of one homogenizer and one more attritor mill.[62] This expansion allowed the size of the powder lot to be increased from 50 kg MOX to 150 kg MOX with additional benefits such as reducing the number of quality control points and operating with a larger quantity of fuel with uniform plutonium isotopic composition.[9] After conditioning in the spheroidizer, the powder is pelletized into green pellets using a hydraulic multipunch press, and then green pellets are sintered at temperatures of up to 1750°C under an atmosphere of $Ar + 4\%$ H_2 mixture gas without heat treatment in a dewaxing furnace.[63] An automatic pellet inspection system is adopted for monitoring each pellet diameter, pellet surface, and end surfaces after centerless grinding.[8] The MOX pellets produced by the SBR process have a mean grain size of about 7.4 μm with a standard deviation of 0.6 μm, and mean pore diameter is about 5 μm.[62]

2.01.5.2.6 Developments for future systems

In order to improve the economical aspects of MOX pellet fabrication and to extend the fabrication process to MOX pellets containing MAs, various R&D programs have been started especially in France, Germany, Japan, and Russia.

In France, several coconversion processes have been developed and combined with the development of reprocessing processes. One typical coconversion process, called the CO-EXtraction (COEX) process, has been developed at the ATALANTE (Atelier Alpha et Laboratoires d'Analyses des Transuraniens et d'Etudes de Retraitement).[58,64] In this, a mixture of uranyl and plutonium nitrate solutions containing MAs is coconverted to MOX powder following the oxalate precipitation method. According to the results of
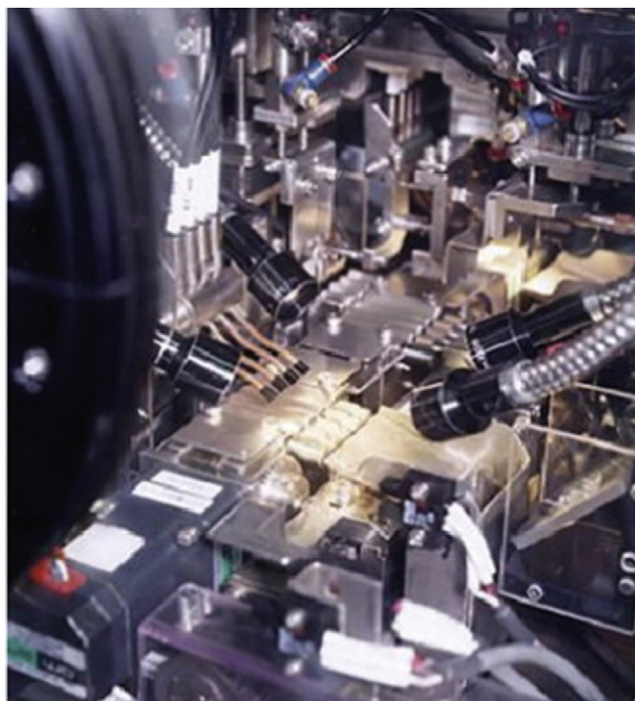
Fig. 28 Inspection device for pellet density and appearance.

COEX pellet fabrication tests in the MELOX test chain, MOX pellets produced by the COEX process have mean grain size larger than 6 μm. These are compatible with current MOX manufacturing values obtained in the MELOX.[58] In parallel with the above development, fuel fabrication processes have also been developed in the ATALANTE and LEFCA (Laboratoire d'Etudes et de Fabrications Experimentales de Combustibles Nucleaires Avances).

In Germany, basic R&D concerning fabrication processes for MOX fuel bearing MAs have been carried out at the Institute for Transuranium Elements (ITU now JRC).[65] One of the fuel irradiation test programs carried out by JRC was the SUPERFACT experiment. In this experiment, SUPERFACT fuels bearing Np or Am were fabricated by the sol–gel method and they were irradiated in various fast reactors.[14,65]

In Japan, a simplified MOX pellet fabrication process, the short process, has been developed on the basis of the MH method, for the above purposes. The flow sheet for this process is shown in **Fig. 30**. A 300 g scale laboratory test of the short process has been successfully completed.[66]

In the short process, three different solutions, uranyl nitrate, plutonium nitrate, and a nitrate solution in which rejected MOX pellets are dissolved, are mixed to obtain the desired plutonium content in the final mixed solution. Then, the mixed solution is converted to the MH-MOX powder with desired plutonium content by the MH method. This converted MH-MOX powder is tumbling-granulated after adding an adequate amount of water as a binder to improve its flowability. The tumbling-granulated MH-MOX powder is calcined at 750°C in air and reduced to MH-MOX powder at 750°C under an atmosphere of N_2 + 5% Ar mixed gas. The MH-MOX powder so obtained is directly pressed into green annular pellets using a die-wall lubrication method. These are then sintered without heat treatment in the dewaxing furnace because the amount of organic compounds contained in the green pellets is controlled at a lower value than that in pellets prepared by the conventional MOX fuel fabrication process. Sintered MOX pellets are ground by a centerless grinder, and subsequently, the geometrical density and appearance of each pellet are inspected. The MOX pellets rejected at the inspections are dissolved in nitric acid and used as part of the final blending solution as shown in **Fig. 30**. **Fig. 31** shows a photograph of annular MOX pellets prepared by the short process. A ceramograph of a pellet prepared by the short process is shown in **Fig. 32**.

The MOX pellets manufactured by the short process have a larger mean grain size than those manufactured by the other processes such as the SBR, MIMAS, JAEA, and COEX processes. The development of a series of small scale (kg scale) test devices was started in 2007.[14] In parallel with this work, JAEA has an irradiation test program for MOX pellets bearing MAs, to understand their irradiation behavior. In this program, MOX pellets bearing the MAs, Am, and Np were prepared by the JAEA process and irradiated in JOYO. These irradiated pellets were subjected to post-irradiation examinations and the results obtained have been reported in Maeda *et al.*[67,68]

In Russia, RIAR (Research Institute of Atomic Reactors) has proposed the demonstration program concept DOVITA (Dry reprocessing, Oxide fuel, Vibropac, Integral, Transmutation of actinides) and many R&D activities related to them have been carried out. From this program, vibro-packing technology has been applied to load MOX granules into a cladding tube.[69,70]
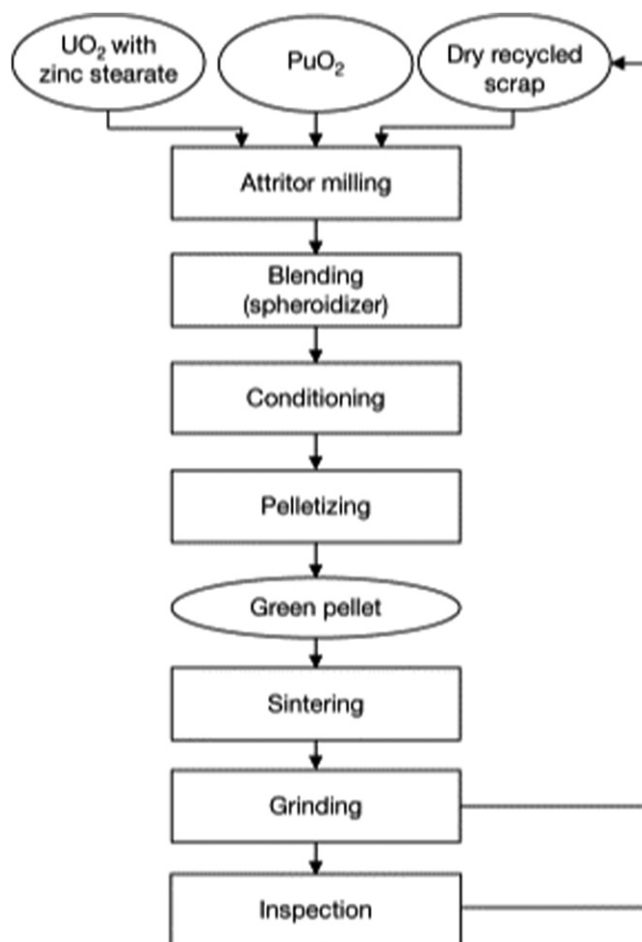
Fig. 29 Flow sheet for short binderless route process.

2.01.6   Rod Fabricating and Assembling

2.01.6.1   LWR UO$_2$ and MOX Fuels

The LWR fuel designs are described in Section 2.01.5.2.2. There are some differences in the fuel assembly fabrication process between PWRs and BWRs. On the other hand, there is no major difference between UO$_2$ and MOX with respect to the fuel assembly fabrication. As an example, the flow sheet of PWR fuel assembly fabrication is shown in Fig. 33.

2.01.6.1.1   Rod fabrication
The fabrication of LWR fuel rods involves the introduction of fuel pellets and a spring into the cladding tube, followed by welding of the end plugs and the cladding tube. For PWRs, the rods are filled with helium at a higher pressure than for BWRs. For this purpose, the top plug has a hole through which the fuel rod is pressurized, and then the hole is arc-welded. The fuel rods are inspected for surface contamination, dimensions, appearance, plug welds, leak tightness, and uranium enrichment by gamma scintillation spectrometry. The fabrication and inspection operations are highly automated and use advanced inspection technologies, such as an X-ray image digitizing system.

2.01.6.1.2   Assembly fabrication
The PWR fuel assembly consists of fuel rods, grids, the top nozzle, the bottom nozzle, the instrumentation tube, and guide tubes. First, the skeleton assembly is made, which is an assembly of the instrumentation tube and the grids. Then, the fuel rods and the guide tubes are inserted into the skeleton assembly. Finally, the top nozzle and the bottom nozzle are mounted on the guide tubes by screws.

The BWR fuel assembly consists of fuel rods, water rods, grid spacers, the upper tie plate and the lower tie plate. First, the water rods, grid spacers, and the lower tie plate are assembled. Then, fuel rods are inserted into grid spacers and tie rods are connected to the lower tie plate. Finally, the upper tie plate is mounted and connected to the tie rods with screws.
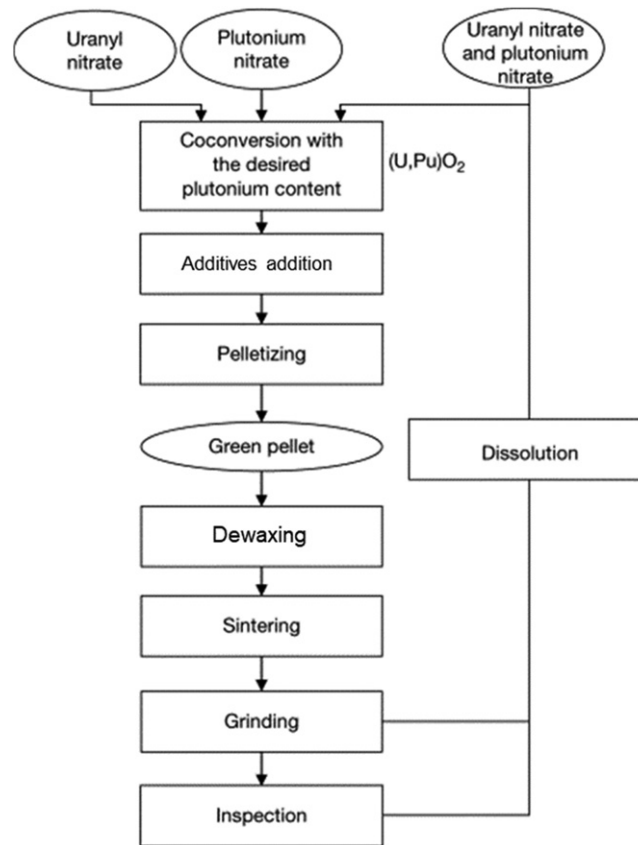
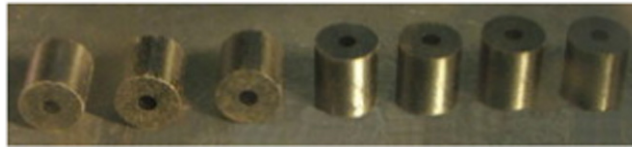**Fig. 30**   Flow sheet for the short process.

Fig. 31   Photograph of annular mixed oxide of uranium and plutonium pellets prepared by the short process (outer diameter: ∼7 mm, height: ∼8 mm, diameter of center hole: ∼2 mm).

The dimensions and appearance of the fuel assemblies are inspected and the BWR fuel assembly is attached to the channel box before loading it into a reactor.

2.01.6.2   Fast Spectrum Oxide Fuel Reactors

As described in Section 2.01.3.2.7, two types of pin spacing for fuel assemblies, the grid type and the wire type, have been adopted for all FBRs. The wire type is more widely used except the Dounreay Fast Reactor in UK.[33] Here, the rod fabrication and assembly are described taking a wire spacer type fuel assembly from the MONJU as an example.

The lower end plug is TIG-welded (tungsten inert gas-welded) to a cladding tube made of SUS 316 based alloy; this is done outside the PFPF. Cladding tubes with lower end plugs are then transferred to PFPF along with blanket pellets of depleted UO_2 and the other cold components such as plenum sleeves and plenum springs. After adjusting the column length of MOX pellets and measuring their weight, they are loaded into each cladding tube with the other components; this is done in a glove box under a helium gas atmosphere. Then, an upper end plug is TIG-welded to the cladding tube. In this welding, the position of the weld electrode is adjusted automatically using image analysis. **Fig. 34** shows photographs of a welding torch installed in the glove box and an image display showing the position of the weld electrode.

Decontamination of the fuel rod surface is carried out prior to a contamination check. The fuel rods which pass the contamination check are brought from the glove box and are sent to the helium leak test to certify tightness of the welded part. An X-ray check of the welded part to confirm its soundness is also carried out prior to wrapping a spacer wire around the fuel rod.
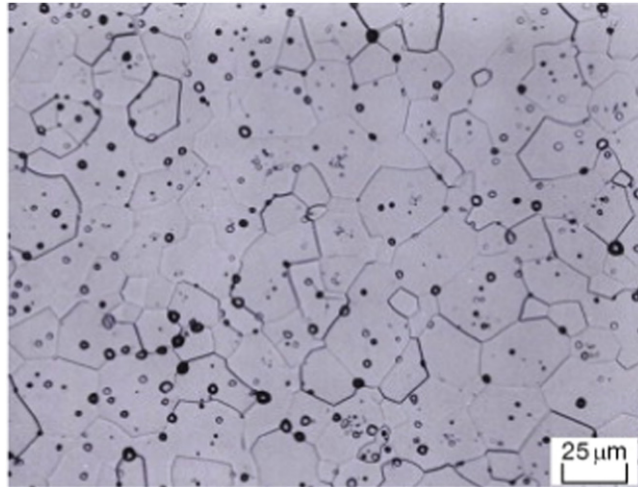
Fig. 32 Ceramograph of a transverse section of a mixed oxide of uranium and plutonium pellet prepared by the short process (plutonium content: 30.0 wt%, density: 96.72% theoretical density, mean grain size: 14 μm).
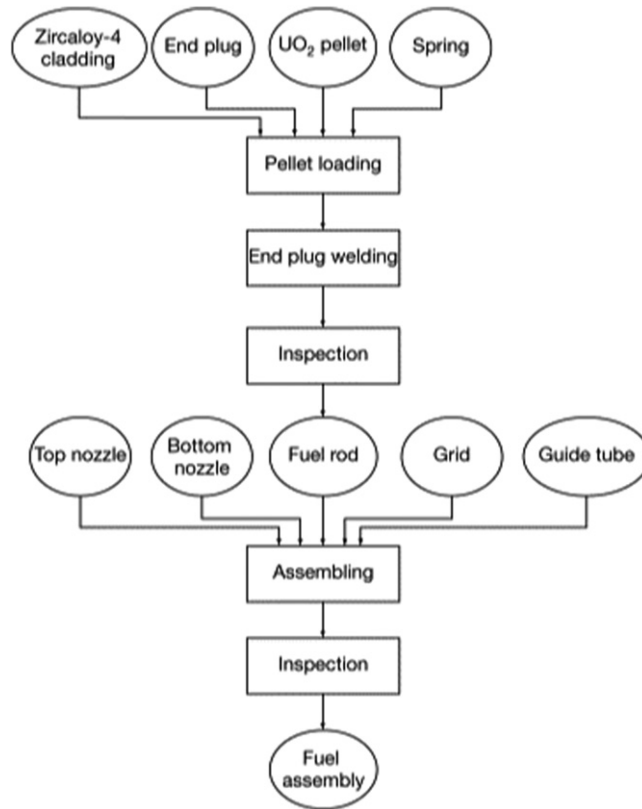

Fig. 33 Flow sheet for pressurized water reactor fuel assembly fabrication.

Finally, each fuel rod is checked for its weight, straightness, gap between spacer wire and fuel rod, γ-ray spectrum from Am in the MOX pellets, and general surface appearance. Next, 169 fuel rods are transferred to the automated assembly station where 15 layers of fuel rods, consisting of 8–15 rods in each layer, are prepared at first. The layers of fuel rods are fixed to the entrance nozzle one by one to get a hexagonal cross-section. This bundle of 169 fuel rods is inserted into a wrapper tube, and then this wrapper tube is TIG-welded to the entrance nozzle.

Fig. 35 shows a photograph of a bundle being inserted into a wrapper tube at the assembly station. The completed fuel assembly is then moved to an inspection station to confirm its straightness, twist, distance between opposite outer surfaces and appearance through automatic and remote operations.
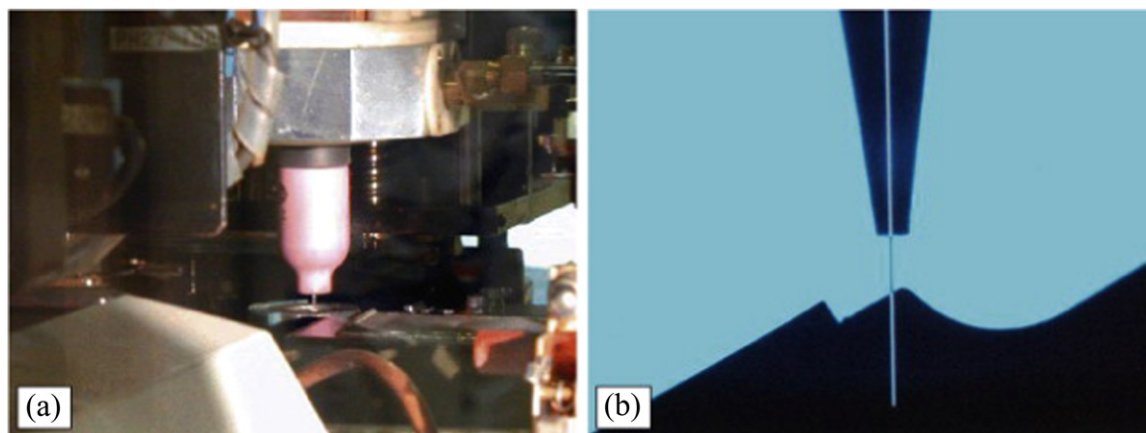
Fig. 34   Photographs of (a) a welding torch and (b) an image display showing the position of the weld electrode.
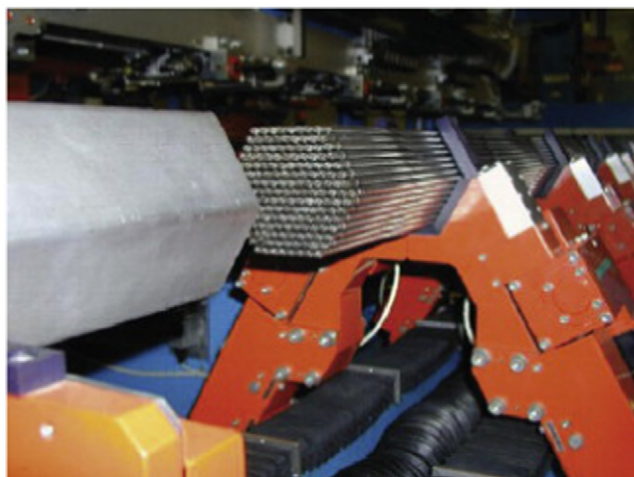

Fig. 35   Photograph of assembling station for FBR assembly.

2.01.7   Outlook

The international market of LWR uranium-oxide fuels has been already established. A supply of economical and high-performance fuels is sought under the condition of conformance to safety requirements of each country. The high burnup fuel is one of the most important targets. Several cladding materials with improved corrosion resistance have been developed. In the field of fuel development, fuel pellets of which fission gas release rate is low have been required.

MOX fuels have been used successfully in several countries in which the fuel cycle policy is adopted to manage the spent fuel adequately. There is no specific challenge of MOX fuel in the fuel performance of reactor safety. Some improvements in the MOX fuel fabrication are required to keep the economic competitiveness, mitigating the effect of strict control of plutonium handling.

Hydrogen gas was generated in the severe accident which occurred in the Fukushima Daiichi nuclear power plant in 2011 by the reaction between Zircaloy cladding and coolant water in the very high temperature. Hydrogen explosion caused the expanded release of radioactive materials to the environment. Some new cladding materials which will not produce hydrogen gas during severe accidents are under development for ATFs (accident tolerant fuels).

Fast reactors can burn effectively minor actinide (MA) elements which have a long decay period and high heat generation feature. The heat generation of the vitrified high-level radioactive wastes is reduced by eliminating MA from the wastes. It enables area reduction of the geological disposal repository. The development of MA-containing fuels is indispensable to achieve the MA recycle system. Accomplishment of remote-control technology, simplification of fabrication process and enhancement of radiation resistant equipments will be necessary to fabricate MA-containing fuels which have a high radioactivity and a high heat generation.

Nuclear innovation including development of new reactor systems is expected to make nuclear energy more attractive. Technical innovation should be sought in the field of fuel development and fuel fabrication.

References

1. World Nuclear Association, 2009. World Nuclear Power Reactors 2007–2009 and Uranium Requirements. World Nuclear Association. Available at: http://www.world-nuclear.org/info/reactors.html.
2. IAEA, 2003. Status and Advances in MOX Fuel Technology. Technical Reports Series No. 415. Vienna: IAEA.
3. Kato, M., Morimoto, K., Sugata, H., et al., 2008. J. Nucl. Mater. 373, 237–245.
4. Sari, C., Benedict, U., Blank, H., 1970. J. Nucl. Mater. 35, 267–277.
5. Komeno, A., Kato, M., Uno, H., et al., 2010. IOP Conf. Ser.: Mat. Sci. Eng. 9, 012016.
6. Kato, M., Konashi, K., 2009. J. Nucl. Mater. 385, 117–121.
7. Takeuchi, K., Kato, M., Sunaoshi, T., Aono, S., Kashimura, M., 2009. J. Nucl. Mater. 385, 103–107.
8. MacLeod, H.M., Yates, G., 1993. Nucl. Technol. 102, 3–17.
9. Bariot, H., Van Vliet, J., Chiarelli, G., et al., 2000. MOX fuel cycle technologies for medium and long term deployment. In: Proceedings of an International Symposium Held in Vienna, Austria, 17–21 May 1999, pp. 81–101. Vienna, Austria: IAEA.
10. Krellmann, J., 1993. Nucl. Technol. 102, 18–28.
11. Carr Jr., R.L., 1965. Chem. Eng. 163–168.
12. ASTM International, 2006. Standard Test Method for Solid Characteristics by Carr Indices. ASTM D 6393-99. West Conshohocken, PA: ASTM International.
13. Asakura, K., Kato, Y., Furuya, H., 2008. Nucl. Technol. 162, 265–275.
14. Asakura, K., Takeuchi, K., Makino, T., Kato, Y., 2009. Nucl. Technol. 167, 348–361.
15. Kato, M., Watanabe, M., Matsumoto, T., Hirooka, S., Akashi, M., 2017. J. Nucl. Mater. 487, 424–432.
16. Besmann, T.M., Lindemer, T.B., 1985. J. Nucl. Mater. 130, 489–504.
17. Takeuchi, K., Kato, M., Sunaoshi, T., 2011. J. Nucl. Mater. 414, 156–160.
18. Woodley, R.E., Gibby, R.L., 1973. HEDL-SA-592.
19. Suzuki, K., Kato, M., Tamura, T., Aono, S., Kashimura, M., 2007. J. Alloys Compd. 444–445, 590–593.
20. Oak Ridge National Laboratory, 1965. Dissolution of High-Density UO_2, PuO_2, and UO_2–PuO_2 Pellets in Inorganic Acids. ORNL-3695. Oak Ridge, TN: Oak Ridge National Laboratory.
21. Oak Ridge National Laboratory, 1968. Preparation and Properties of Actinide Oxides. ORNL-4272. Oak Ridge, TN: Oak Ridge National Laboratory.
22. Lerch, R.E., 1979. Dissolution of Mixed Oxide Fuel as a Function of Fabrication Variables. HEDL-SA-1935. Windscale, UK: US/United Kingdom Information Exchange on Dissolution of Nuclear Fuel.
23. Crofts, J.A., Douglas, J.A.M., Weatherley, L.R., Wilkinson, K.L., 1980. Proceedings of a Symposium Sponsored by the Society of Chemical Industry, Dounreay, UK, May 15–18, 1979, pp. 149–168. London: Society of Chemical Industry.
24. Shibata, K., Kawano, T., Nakagawa, T., et al., 2002. J. Nucl. Sci. Technol. 39, 1125–1136.
25. Hori, M., 1993. Kiso Kousokuro Kougaku (Basic Fast Reactor Engineering). Tokyo: The Nikkan Kogyo Shimbun, (in Japanese).
26. Nakae, N., 2006. J. Nucl. Sci. Technol. 43, 361–366.
27. Cahn, R.W., Haasen, P., Kremer, E.J. (Eds.), 1994. Materials Science and Technology, vol. 10A: A Comprehensive Treatment. Weinheim, Germany: VCH (Verlagsgesellschaft mbH).
28. Bailly, H., Menessier, D., Prunier, C. (Eds.), 1999. The Nuclear Fuel of Pressurized Water Reactors and Fast Reactors. Paris: CEA.
29. Olander, D., 2009. J. Nucl. Mater. 389, 1–22.
30. Tarlton, S., 2008. Nucl. Eng. Int. 53, 26–36.
31. Lawrence, L.A., Jensen, S.M., Hales, J.W., Karnesky, R.A., Makenas, B.J., 1986. International Conference on Reliable Fuels for Liquid Metal Reactors, Tucson, AZ, September 7–11, 1986, pp. 3-62–3-74. La Grange Park, IL: American Nuclear Society.
32. Department of Energy, National Nuclear Security Administration, 2002. Amended Record of Decision for the Surplus Plutonium Disposition Program, 67 FR 76, April 19, 2002. Washington, DC: Office of the Federal Register.
33. Arslan, M., de Villèle, E., Gauthier, J.-C., Marincic, A., 2013. MOX recycling in GEN 3+ EPR reactor, homogeneous and stable full MOX core. In: Proceedings of the GLOBAL 2013: International Nuclear Fuel Cycle Conference – Nuclear Energy at a Crossroads, Salt Lake City, UT (United States).
34. IAEA, 2006. Fast Reactor Database 2006 Update. IAEA-TECDOC-1531. Vienna: IAEA.
35. Assman, H., Becker, M., 1979. Trans. Am. Nucl. Soc. 31, 147–148.
36. Heal, T.J., Littlechild, J.E., 1978. Trans. Am. Nucl. Soc. 28, 326–328.
37. Assman, H., Bairiot, H., 1983. Technical Report Series No. 221. Vienna: IAEA, pp. 161–166.
38. Hirai, M., Hosokawa, T., Yuda, R., et al., 1997. Proceedings of the International Topical Meeting on LWR Fuel Performance, Portland, OR, March 2–6, 1997. La Grange Park, IL: American Nuclear Society.
39. Bourgeois, L., Dehaudt, P.H., Lemaignan, C., Hammou, A., 2001. J. Nucl. Mater. 297, 313–326.
40. Harada, Y., 1997. J. Nucl. Mater. 245, 217–223.
41. Assmann, H., Peehs, M., Roepenack, H., 1988. J. Nucl. Mater. 153, 115–126.
42. Burkes, D.E., Fielding, R.S., Porter, D.L., Meyer, M.K., Makenas, B.J., 2009. J. Nucl. Mater. 393, 1–11.
43. Kittel, J.H., Frost, B.R.T., Mustelier, J.P., et al., 1993. J. Nucl. Mater. 204, 1–13.
44. Boltax, A., 1994. In: Cahn, R.W., Haasen, P., Kremer, E.J. (Eds.), Materials Science and Technology: A Comprehensive Treatment 10B. New York: VHC, pp. 341–390.
45. Mignanelli, M., Potter, P.E., 1986. Proceedings of the BNES International Conference on Science and Technology of Fast Reactors Safety, Guernsey, UK, May 12–16, 1986, vol. 1, pp. 53–57. London: British Nuclear Energy Society.
46. Mignanelli, M., Potter, P.E., 1988. Thermochim. Acta 129, 143–160.
47. Strain, R.V., Bottcher, J.H., Ukai, S., Arii, Y., 1993. J. Nucl. Mater. 204, 252–260.
48. OECD NEA, 1997. Management of Separated Plutonium – The Technical Options. Paris: OECD NEA.
49. Haas, D., Vandergheynst, A., Lorenzelli, R., Nigon, J.L., 1994. Nucl. Technol. 106, 60–82.
50. Cleveland, M.J., 1979. The Chemistry of Plutonium. La Grange Park, IL: American Nuclear Society.
51. Koizumi, M., Ohtsuka, K., Isagawa, H., Akiyama, H., Todokoro, A., 1983. Nucl. Technol. 61, 55–70.
52. Oshima, H., 1989. J. Sci. Technol. 26 (1), 161–166.
53. Kato, Y., Kurita, T., Abe, T., 2004. J. Sci. Technol. 41 (8), 857–862.
54. Kato, Y., Kurita, T., Abe, T., 2005. Trans. Jpn. Nucl. Soc. 4 (1), 77–83. (in Japanese).

55. Oudinet, G., Munuz-Viallard, I., Aufore, L., *et al.*, 2007. J. Nucl. Mater. 375, 86–94.
56. Bouloré, A., Aufore, L., Federici, E., Blanpain, P., Blachier, R., 2015. Advanced characterization of MIMAS MOX fuel microstructure to quantify the HBS formation. Nucl. Eng. Des. 281, 79–87.
57. Garcia, P., Bouloré, A., Guérin, Y., Trotabas, M., Goeuriot, P., 2000. Proceeding of the International Meeting on Light Water Reactor Fuel Performance, CD-ROM, Park City, UT, April 10–13, 2000. Park City, UT: American Nuclear Society.
58. Roepennack, H., Shhlemmer, F.U., Schlosser, G.J., 1986. Nucl. Technol. 77, 175–186.
59. Okita, T., Aono, S., Asakura, K., Aoki, Y., Ohtani, T., 2000. MOX fuel cycle technologies for medium and long term deployment. In: Proceedings of an International Symposium Held in Vienna, Austria, May 17–21, 1999, pp. 109–117. Vienna, Austria: IAEA.
60. Asakura, K., Yamaguchi, T., Ohtani, T., 2007. J. Nucl. Mater. 357, 126–137.
61. Edwards, J., Brown, C., Marshall, S., Connell, M., Thompson, H., 1999. Proceedings of the Fifth International Conference on Recycling, Conditioning and Disposal – RECOD 98, Nice, France, October 25–28, 1998, pp. 182–190. Paris: SFEN (French Nuclear Society).
62. Grandjean, S., Arab-Chapelet, B., Robisson, A.C., *et al.*, 2007. Synthesis of mixed actinide compounds by hydrometallurgical co-conversion methods. In: Proceedings of the Global 2007, Advanced Nuclear Fuel Cycles and Systems, Boise, ID, September 9–13, 2007, pp. 98–105.
63. IAEA, 1995. Recycling of plutonium and uranium in water reactor fuel. In: Edwards, J., Crimoldby, R.D., Marshall, S.J., Stratton, R.W. (Eds.), BNFL Supply of MOX Fuel Assemblies to the Beznau 1 PWR of NOK. IAEA-TECDOC-941. Vienna: IAEA, pp. 57–67.
64. Fernandez, A., Mcginley, J., Somers, J., Walter, M., 2009. J. Nucl. Mater. 392, 133–138.
65. Prunier, C., Boussard, F., Koch, L., Coquerelle, M., 1997. Nucl. Technol. 119, 141–148.
66. Ito, M., Funasaka, H., Namekawa, T., 2007. European Nuclear Conference (ENC) 2007, Brussels, Belgium, September 16–20, 2007, Brussels: ENC.
67. Maeda, K., Sasaki, S., Kato, M., Kihara, Y., 2009. J. Nucl. Mater. 389, 78–84.
68. Herbig, R., Rudolph, K., Lindau, B., Skiba, O.V., Maershin, A.A., 1993. J. Nucl. Mater. 204, 93–101.
69. Bychkov, A.V., Skiba, O.V., Mayorshin, A.A., *et al.*, 2002. Burning of minor actinides in fuel cycle of the fast reactor: DOVITA programme-results of the 10 year activities. In: Proceedings of the 7th Information Exchange Meeting on Actinide and Fission Product Partitioning and Transmutation, Jeju, Republic of Korea, October 14–16, 2002, pp. 295–307.
70. Burkes, D.E., Fielding, R.S., Porter, D.L., Crawford, D.C., Meyer, M.K., 2009. J. Nucl. Mater. 389, 458–469.

Relevant Website

http://www.mhi.co.jp/en/index.html
   Mitsubishi Heavy Industries, Ltd. Global Website.